IEEE Transactions ON AUDIO

Formerly IRE Transactions on Audio

Volume AU-11 JANUARY-FEBRUARY, 1963 Number 1

Published Bi-Monthly

TABLE OF CONTENTS

PROFESSIONAL TECHNICAL GROUP ON AUDIO

The Editor's Corner

INTERRUPTIONS

Tuesday morning Joe Zilch, Senior Audio Engineer, arrived at the office 7:30 A.M. to carry out his New Year's resolution. This year he would "get organized" and concentrate on really important engineering work. Joe believed, and it was the policy of his company, that good engineers should be encouraged to do engineering, rather than be promoted to paper work.

The quietness at this early hour gave Joe the feeling that it was ten years ago and he was back in his first lab. In those days nobody knew him. He was not on any mailing lists. The telephone seldom rang. All day long he could work, and read, and think about his work. "Why can't I set back the clock to those days," thought Joe, "I used to get quite a bit done. Nowadays it's all these darned interruptions. On a new problem it takes me at least fifteen minutes to collect my thoughts. But somebody bothers me every five minutes, so I never settle down."

It occurred to Joe that here was a nonengineering problem, but one which was more important than the technical problems, because he would have to solve it before he could be effective at engineering again. Then Joe got an idea. He would keep track of all interruptions that day. On a large sheet of paper he marked a column UI for *unnecessary interruptions*, another column NI for *necessary interruptions* which could not be avoided.

While everything was quiet Joe made some notes on an experiment he had wanted to carry out in the past two years. He set up the equipment and was ready to take readings by 9:30 A.M. Now it was breakfast coffee time; Bill and George were waiting. Joe didn't particularly want coffee, but he didn't want to appear unfriendly. Anyway he might learn something from the discussion. The discussion was nontechnical and it only seemed like fifteen minutes, but Joe noticed it was 10:20 when he got back.

"Don't know where the time went," thought Joe, as he wrote it in the UI column of his score card. Then he rationalized, "A fellow does have to eat. And one can't be a hermit." He transferred the item to the NI column, with a note about shortening the time.

On Joe's desk was a memo of three phone numbers that had called, one from home. He phoned his home first. Line busy. Try again later. The other two parties were out. As Joe was remembering what he was to do next on his experiment, the phone rang. A person had bought a used obsolete amplifier made by the company. Wanted advice on how to modernize it. The call had been transferred four times. Joe listened patiently, and gave his opinion. Had to be nice to enhance the company's image.

Reluctantly Joe entered the time as NI. "When the telephone rings you must drop what you are doing, no matter how important, and must listen to what your party says, no matter how trivial. Politeness requires it. But no one ever considers a caller impolite."

Now back to taking readings. There was a knock on the door and in came J.P., the Vice President in charge of research. Joe brought him up to date on the various projects, and J.P. appeared satisfied. "There are a few matters," said J.P., "and maybe someone else could handle them. But when something is important you are the only one I can depend on to do it right. It's easier for you than for the others because you have the know-how and you don't waste time."

Joe was warmed by the compliment, but as J.P. elaborated he cringed inwardly. The weekly seminar: an eminent person like Joe himself ought to introduce the speakers, and couldn't Joe invite some top scientists to speak? The new research center needed planning so that mistakes of the present one would not be repeated and new mistakes would be avoided. The architect might come this afternoon for a discussion and would leave a set of prints for Joe to work on. The high school science fair needed an adult advisor; our company should cooperate; it's only an hour a week. And finally, the fall audio convention needs papers. Could he encourage some junior engineers, or even write one himself?

J.P. left and Joe thought, "There went the rest of the morning." Into the NI column. You can't shut the door on J.P.

Lunch time. Joe planned a brief meal, but after lunch the boys visited Matt Smith, who was in the hospital recovering from an automobile accident. Matt was a good friend and Joe went along. At 1:30 it looked as if the group would be there all afternoon. Joe excused himself and drove back to the laboratory by himself. He marked an extra hour in the NI column. Only a selfish person would dodge human and social obligations.

On his desk was the afternoon mail. First Joe opened the "real" letters as he was curious to know what they said. All of them required answers. He put these to one side. Next the junk-mail. Most of it went into the wastebasket, but he saved a few items that might come in handy. How could he file them so they would be found when needed? Information retrieval was a big problem. Finally the technical journals. He took a quick glance through the thin ones. The thick ones were hopeless. With a sigh he put them on top of the ever growing pile of journals he intended to read but now knew he never would. Do the best engineers keep up with the literature? Joe sort of doubted it. He had a suspicion that those who wrote articles for journals were too busy writing to do much reading. The letter opening ritual was duly recorded as an NI. A secretary could help, but most of the items needed personal decision.

Suddenly, Joe remembered his experiment. He turned on the equipment, and sure enough, in came Al and Pete. "Would you like to see something?" Al asked, "Come down the hall." A minute later they were trying a new demonstration built for the trade show. Joe made a few suggestions and headed back for his room.

Waiting at his door was Bob. "You know that test rig you designed; it won't work at all," Bob accused. "Would you like to look at it? We tried it six ways. Should have built it differently." In the main lab they turned on the set; it squealed at a 120-db level. Joe traced the circuit. The negative feedback was reversed and the chassis wasn't grounded. After they had fixed the main trouble there was still a bit of hum to clean up. Joe explained in detail how to trace ground-loops.

Back in his office Joe considered that he ought to prepare mimeographed sheets for things that occurred over and over again. But long ago he learned that you can't make anything foolproof, because as you improve it, the fools are also improving and they find better ways to outwit you.

Into the NI column went *Technical Consultation*. An important obligation of a senior scientist was to give advice and counsel to the junior ones. But they could keep a good engineer so busy with their elementary troubles that he was never able to get to his own advanced troubles.

The clock now said 4:45. Just time enough to make out the time sheets, sign the letters, lock the cabinets, and join the rat-race going home. For a moment Joe thought that he might stay overtime and take some readings. Impossible tonight; he was host for the bridge club. Same situation every night this week, in fact.

Joe wrote down this last NI of the day at 4:58. The UI column was still blank. His important experiment had not been touched.

As Joe rode home that night he reflected that here was a typical day when he was not under pressure. There had been no conferences, no outside visitors, no talks to prepare, no deadlines on reports, no production emergencies. It was painfully clear that if he hadn't found uninterrupted research time today, he probably never would.

MARVIN CAMRAS, *Editor*

PGA News

CHAPTER NEWS

Cincinnati, Ohio

"Development of the Baldwin Three-Manual Organ" was presented by Albert Meyer, Supervisory Research Engineer of the Baldwin Piano Company, at 8:00 P.M. on Tuesday, January 15, 1963.

The basic system research and development which led to the Baldwin three-manual organ was described. Afterward Mr. Meyer played a demonstration recital on a production organ of this type.

This meeting was held at the organ demonstration room of the Baldwin Piano Company, Plant No. 3, 2045 Gilbert Avenue. All IEEE Section members, their wives, and other engineers were invited to this program of outstanding technical and musical interest.

Albert Meyer (S'46–A'51–M'52–SM'55) received the B.S.E.E. and M.S.E.E. degrees from the University of Cincinnati, in 1948 and 1950, respectively. He joined the Engineering Staff of The Baldwin Piano Company in 1950. Since that time, in addition to numerous engineering accomplishments in electronic organ design, he has participated in the development of high-powered audio systems for airborne applications.

Mr. Meyer is a member of Eta Kappa Nu, Tau Beta Pi, and Sigma Xi. He is Past Chairman of the Cincinnati IRE Section administration. He is currently Dean of the Cincinnati Chapter of the American Guild of Organists.

He holds several patents and has authored a number of papers and articles on audio subjects. He was corecipient of the PGA Award in 1956.

Report on Budapest Conferences on Signal Recording

An international "Conference on Signal Recording on Moving Magnetic Media," sponsored by the Hungarian Society for Optics, Acoustics and Filmtechnics, was held in Budapest, October 15–18, 1962. The meeting was attended by 220 engineers, scientists, and technicians, from six socialist and eight nonsocialist countries. The preponderance of attendees were from Budapest, as might be expected. The only attendees from the USA were Dr. Peter Goldmark and Donald F. Eldridge. Forty-seven technical papers were presented—14 from "Western" countries and 33 from socialist countries. There were no technical papers and only two attendees from the USSR.

It was interesting to find a great deal of work being done on magnetic recording in the socialist countries. Most of the effort appears to be in hardware building, in which they seem to be several years behind the West. Most of the theoretical and advanced-state-of-the-art papers were from the West. That is not to say the Eastern Europeans are not doing good work—they are, and are making good progress. But they have a lot of equipment to build before they can concentrate on real advances in the art, either theoretically or experimentally. The proceedings of the conference will be published sometime in 1963.

During the conference a meeting was held among a small group of participants from 10 countries to discuss the desirability and feasibility of holding future conferences on the same subject. A temporary commission was elected to coordinate further efforts in this direction. The committee is composed of Gabor Heckenast of Hungary, Chairman, and Dr. Schiesser of West Germany, Professor Nagai of Japan, and D. F. Eldridge of the U.S.A. A member from the USSR is to be appointed later. This commission then agreed to study the possibilities of and interest in another conference with other technical men in their own geographical area. It was agreed that it would be desirable to hold another conference in about three years, in a location yet to be determined.

Anyone having suggestions to make concerning a future conference is invited to contact D. F. Eldridge, Memorex Corporation, 1180 Shulman Avenue, Santa Clara, Calif.

A Special Application of Information Theory to Recording Systems*

DONALD F. ELDRIDGE†, SENIOR MEMBER, IRE

Summary—Information theory concepts are applied to determine storage capacity and efficiency of recording media and techniques. Because the signal-to-noise ratio is a function of track width, the capacity must be calculated on an area basis. Expressions are derived for the storage capacity as a function of track width and number of levels stored. This provides a means for comparing the efficiency of various recording techniques such as binary digital, multilevel digital and analog. The results are: 1) The maximum information storage capacity of a recording medium can be determined and the degree to which a practical recording system approaches this can be calculated. 2) The information capacity per unit width of tape or per unit area is greatest when the tracks are made as narrow as possible. 3) Binary recording is more efficient than any digital system using a higher numerical base if very narrow tracks can be utilized. 4) When track width is determined by mechanical factors, multilevel digital storage may be most efficient. The optimum number of levels may be calculated from the signal-to-noise ratio of the track. 5) Binary recording is much more efficient than analog recording when high accuracies or large signal-to-noise ratios are desired.

Storage Capacity of a Recording System

IN APPLYING information theory to magnetic recording, it is usual to consider the recorder channel as an ordinary communications channel with fixed signal-to-noise ratio. This is a useful concept and may be used to determine optimum coding systems for a given recorder channel. In magnetic recording (and in certain other types of recording), however, there is another factor which must be considered: the SNR of a track is a function of its width. Therefore, it is possible to obtain two or more tracks in the place of one, with equal bandwidth and a lower SNR. Hence, the over-all information capacity of a storage medium must be determined on an area basis rather than on a single dimensional basis. This applies to any type of recording in which the SNR is a function of track width.

From Shannon,[1] the capacity in bits per second in a communications channel is

$$C = W \log_2 \left(\frac{S^2 + N^2}{N^2} \right) \tag{1}$$

where W is the bandwidth; S, the rms signal voltage; and N, the rms noise voltage. If this is the capacity of a single track in a recording system, the total capacity per unit width of the tape is

$$C_t = mC \tag{2}$$

where m is the number of tracks per unit width. However, (S^2+N^2/N^2) is a function of the track width d (or $1/m$). Specifically,

$$S/N = \left(\frac{d}{d_0} \right)^{1/2} \tag{3}$$

where d_0 is the track width which will produce a S/N of 1 at the particular bandwidth W. For simplicity, the intertrack spacing is neglected. It may be readily accounted for by assuming it to be a constant percentage of d and d_0, which will not affect the succeeding results. Then, total capacity per unit width, C_t, is

$$C_t = mC = \frac{W}{d} \log_2 \left(1 + \frac{d}{d_0} \right). \tag{4}$$

It can be seen that C_t is a maximum when d in a minimum.

Hence, for

$$d = d_0, \qquad C_t = \frac{W}{d_0} \log_2 (2) = \frac{W}{d_0} \cdot$$

Of course, d_0 is not a constant for a particular medium but is a function of the bandwidth used to define the SNR. For white noise, d_0 is proportional to W and therefore the maximum capacity for a given storage medium is independent of bandwidth. For a typical magnetic tape this figure is approximately 2×10^8 bits per square inch. For the purposes of this paper it is sufficient to say that d_0 is constant for any particular bandwidth. Although it is not usually practical to utilize an SNR of 1, it can be seen from the above that the smaller the track width permissible, the more information can be stored per unit tape width.

For an example, assume $d_0 = 0.01$ mil. (This is a reasonable number if one extrapolates the data in Fig. 5 of Eldridge and Baaba.[2]) Fig. 1 shows the ratio of total capacity per unit width, C_t, to the total capacity using tracks 0.01-mil wide plotted against track width.

* Received November 19, 1962. This paper was presented at the Conference on Signal Recording on Moving Magnetic Media, Budapest, Hungary, October 15–18, 1962.

† Memorex Corporation, Santa Clara, Calif.

[1] C. E. Shannon, "A mathematical theory of communications," *Bell Sys. Tech. J.*, vol. 27, pp. 623–656; October, 1958.

[2] D. F. Eldridge and A. Baaba, "The effects of track width in magnetic recording," IRE TRANS. ON AUDIO, vol. AU-9, pp. 10–15; January–February, 1961.

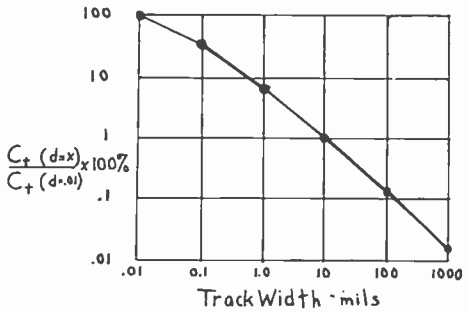

Fig. 1—Information capacity as a function of track width.

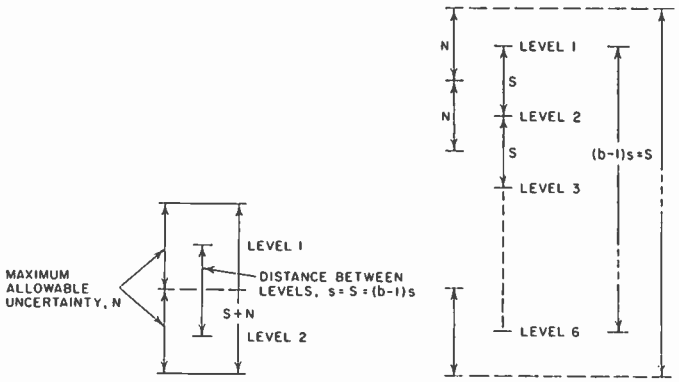

Fig. 2—Illustration of the signal-to-noise as a function of the number of levels. (a) Two-level system. (b) Six-level system.

Effect of Number of Levels Used

The information theory approach can also be utilized to investigate the effects of using different numbers of levels in a recording scheme. This corresponds to using a numerical system, the base of which is the number of levels. Most pulse recording, for example, uses a binary or two-level system. The suggestion has been made from time to time, "Why not use a 3-, 4-, 5-, or some other level system? Wouldn't this produce greater storage efficiency?" Here again, the fact that the SNR is determined by the track width becomes significant.

The SNR required for any number of equally spaced levels may be determined as follows: To specify any given level, the peak-to-peak noise or uncertainty must be just less than the difference between this and the next closest level. This is illustrated graphically in Fig. 2. If b is the number of levels, it determines the total dynamic range required, $S+N$,

$$(S + N) = bN, \qquad S/N = (b - 1). \tag{5}$$

This assumes a noise or uncertainty which never exceeds the specified amount. In practice, of course, the noise signal will have a distribution of peak amplitudes such that, if errors are to be avoided, a value of S/N cannot be based upon the rms noise level. A Gaussian distribution

$$y = (2\pi)^{1/2}e^{-x^2/2}.$$

is a fairly accurate representation of the amplitude distribution of tape noise. Assuming this distribution, there is a probability of 0.32 that the noise will exceed the rms value; a probability of 0.0014 that it will exceed 3.2 (10 db) times the rms value; and a probability of approximately 2×10^{-22} that it will exceed 10 times (20 db) the rms value. To include whatever added S/N is required to give a particular degree of reliability, a factor A will be included such that $S/N = A(b-1)$. Values of A for binary recording have generally ranged from 3.2 to 10, which provide inherent error probabilities as mentioned above. From this value of S/N, the track width required to store digits of any base b may be found and is

$$d = d_0(S/N)^2 = d_0A^2(b - 1)^2. \tag{6}$$

Consider that each track with b levels determines a digit of numerical base b. Then the number of tracks required may be determined from the number of digits D of base b required to specify the number G, as follows:

$$\text{Number of tracks} = D = \log_b G.$$

Hence for any G, the number of tracks required decreases as b increases. The total track width required to store a given number G is then

$$d_t = \text{track width} \times \text{number of tracks},$$
$$d_t = d_0A^2(b - 1)^2 \log_b G. \tag{7}$$

The significance of G is that it is the number of quantized steps or levels which can be recorded and is equal to the resulting over-all SNR computed on a peak-to-peak basis. This is used rather than the peak signal to rms noise used by Oliver, Pierce, and Shannon[3] because it seems to be more physically meaningful.

The peak noise is, of course, the height of a quantizing level and is equal to $1/G$. Now the total track width required to store a number of G using a b-level recording system may be compared with that required by a two-level or binary system. Thus,

$$\frac{d_{t(b)}}{d_{t(2)}} = \frac{d_0(\log_b G)(b - 1)^2}{d_0(\log_2 G)(2 - 1)^2} = \frac{(b - 1)^2}{\log_2 b}. \tag{8}$$

Some values of $d_{t(b)}/d_{t(2)}$ for several values of b are tabulated in Table I. It is apparent, therefore, that because of the SNR requirements any higher level system is inherently less efficient than a two-level system.

In the practical case, however, the minimum track width achievable in a particular recording system may still provide an SNR sufficient for a 3-, 4-, or higher-level system. If this is the case, such as when the track width is limited by mechanical rather than S/N factors, a higher level system will be more efficient.

[3] B. M. Oliver, J. R. Pierce, and C. E. Shannon, "The philosophy of PCM," Proc. IRE, vol. 36, pp. 1324–1331; November, 1948.

TABLE I
VARIABLE S/N

Number of Levels	Track Width Required
b	$d_{t(b)}/d_{t(2)}$
2	1
3	2.5
4	4.5
8	16
10	24
16	56

TABLE II
FIXED S/N

Number of Levels	Track Width Required
b	$d_{t(b)}/d_{t(2)}$
2	1
4	0.5
8	0.33
16	0.25
32	0.20
64	0.17

In this case the relative track width required reduces to

$$\frac{d_{t(b)}}{d_{t(2)}} = (\log_2 b)^{-1}. \tag{9}$$

Several values are tabulated in Table II. The gain in efficiency is not particularly rapid compared to the increase in number of levels. Maximal efficiency occurs when the number of levels reaches the limit imposed by the fixed SNR.

Comparison of Binary and Analog Recording

It has been shown above that binary recording is inherently the most efficient form of digital or quantized recording. Now compare this to unquantized direct or analog recording. The track width required for analog recording can be determined from (7) if it is stated that $G=b$ and that $A=1$. Therefore, the analog track width, d_a, becomes

$$d_a = d_0(S/N)^2 = d_0(G-1)^2. \tag{10}$$

The track width required to specify the same G in binary form may also be determined from (5), and

$$d_d = d_0 A^2 \log_2 G(2-1)^2 = 3.32 A^2 \log_{10} G. \tag{11}$$

In this case, the logarithm base 10 is used to provide easy conversion to decibels. Now to provide a high degree of reliability, assume $A=10$, and that it will require two samples per cycle to specify a sinusoidal signal. These numbers are only illustrative but do give a basis for comparison. Then

$$d_d = d_0(2)(3.32)(100)\log_{10} G = d_0 664 \log_{10} G. \tag{12}$$

Therefore, the ratio of track width required for analog recording to that required for digital recording is

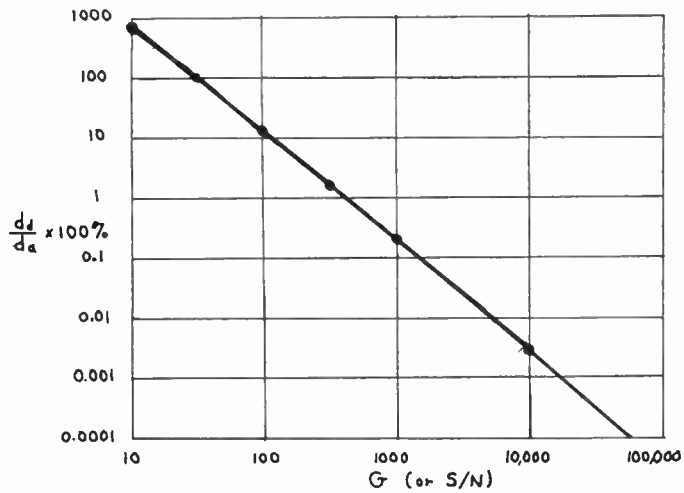

Fig. 3—Relative efficiency of binary digital vs analog recording.

$$\frac{d_a}{d_d} = \frac{(G-1)^2}{664 \log_{10} G}. \tag{13}$$

This ratio is plotted as a function of G in Fig. 3. From Fig. 3, it is apparent that for very small SNR's, direct analog storage is most efficient. However, for high accuracies and large SNR's, binary storage becomes increasingly more efficient. The crossover under these particular assumptions occurs when $S/N=33$. Different values of A and of the number of samples per cycle will merely shift the entire curve up or down by a constant amount and will not change its slope. For example, if $A=3.16$ (a 10-db safety factor), the crossover will occur at $G=9$. Other factors, such as not being able to physically utilize a track width narrow enough to produce the desired value of A will also shift the curve up or down. The fact remains that above the crossover, binary storage becomes more efficient at a rate only slightly less than the square of the actual SNR G.

Conclusions

It has been shown that:

1) The maximum information storage capacity of a recording medium can be determined, and the degree to which a practical recording system approaches this can be calculated.

2) The information capacity per unit width of tape or per unit area is greatest when the tracks are made as narrow as possible.

3) Binary recording is more efficient than any digital system using a higher numerical base if very narrow tracks can be utilized.

4) When track width is determined by mechanical factors, multilevel digital storage may be most efficient. The optimum number of levels may be calculated from the SNR of the track.

5) Binary recording is much more efficient than analog recording when high accuracies or large SNR's are desired.

The implications of this are that to make optimum use of the storage medium, the track widths should be made as small as is practically feasible, and ways should be found to convert the information to be recorded into binary digital form. This applies to all types of information which are presently recorded on magnetic tape. Even information which is now recorded digitally could be recorded more efficiently and with higher accuracy or reliability.

The purpose of this paper has been to introduce a new means for evaluating various recording systems and for guiding the development of new recording techniques. It should be possible to apply these information theory concepts to a wide range of recording problems and to extend the analysis in a number of ways, such as including the effects of amplifier and other noise, volumetric capacity and coating thickness and frequency and wavelength effects.

ACKNOWLEDGMENT

Thanks are due Dr. K. Teer, Philips Research Laboratories, Eindhoven, The Netherlands, and E. D. Daniel, Memorex Corporation, for their valuable corrections and suggestions.

Push-Pull Class-AB Transformerless Power Amplifiers*

L. BLASER†, MEMBER, IRE, AND H. FRANCO†

Summary—**One of the major problems in power-amplifier design is to combine high efficiency with thermal stability. Class-C operation with current drive is one possibility but distortion level is high due to crossover and nonlinearity of h_{FE}. A new diode-compensation method is described which allows high efficiency Class-AB operation for maximum output and lowest distortion and with excellent thermal stability. In the output stage the variation of the quiescent current vs temperature is kept small by a diode-resistance network in the emitter of each driver transistor, thereby eliminating the need for large thermal compensating resistance in the emitters of the output transistors.**

A 10-watt amplifier was designed using the described power-dissipation criteria and the new biasing scheme. Performance of the amplifier demonstrates the effectiveness of the design. It operates with maximum power dissipation up to 65°C ambient with a sine wave input. Calculations are also included in the paper which show the voltage levels of maximum power dissipation for sine, triangular and square waves.

I. INTRODUCTION

THIS PAPER discusses general problems in connection with dissipation, distortion, and thermal stability of transistor power amplifiers. A comparison of distortion between Class-C and Class-AB operation with current and voltage drives shows the advantages of Class-AB operation. A new bias scheme is presented to solve the problem of thermal instability. The results of the Class-AB amplifier analysis, summarized in Section II, can generally be applied to the design of most transistor power amplifiers.

A 10-watt push-pull Class-AB transformerless audio power amplifier was built as a typical application of the design principles presented. Performance of this amplifier is given and its circuit described in Section V.

II. GENERAL DESIGN CONSIDERATIONS OF PUSH-PULL POWER AMPLIFIERS

In a power amplifier, high efficiency requires operation in Class AB, B, or C. For the analysis of power dissipation of the push-pull circuit shown in Fig. 1, let

V_{CC} = supply voltage
V_Q = emitter quiescent voltage
V_{PN} = voltage between the two bases of the transistors
I_Q = quiescent current (zero for Class B or C)
R_L = load resistance.

In the case where $V_Q = V_{CC}/2$ and $I_Q = 0$, the maximum power dissipation in each output transistor, which occurs at other than maximum power output, is given by

$$P_{D\max} \simeq K_D \frac{V_{CC}^2}{R_L}, \tag{1}$$

where K_D is a coefficient given in Table I for three common waveforms.

* Received December 3, 1962; revised manuscript received January 21, 1963.
† Fairchild Semiconductor, a Division of Fairchild Camera and Instrument Corporation, Mountain View, Calif.

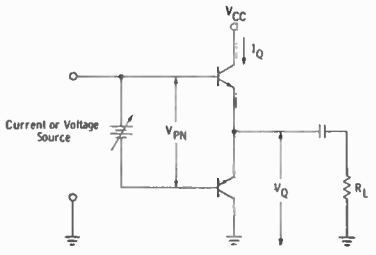

Fig. 1—Push-pull power gain stage of complementary emitter followers.

TABLE I

	Sine Wave	Triangular Wave	Square Wave
K_D	$\frac{1}{4\pi^2}$	0.0235	$\frac{1}{32}$
K_C	2π	6.5	5.6
K_0	$\frac{1}{8}$	$\frac{1}{12}$	$\frac{1}{4}$

This maximum power dissipation should never exceed the permissible dissipation P_P

$$P_{D\max} \leq P_P. \tag{2}$$

The permissible dissipation can be expressed by

$$P_P = \frac{T_{J\max} - T_A}{\theta_{J-C} + \theta_{C-A}}, \tag{3}$$

where

T_A = ambient air temperature
$T_{J\max}$ = maximum permissible junction temperature
θ_{J-C} = thermal resistance between the junction and the case of the transistor
θ_{C-A} = thermal resistance between the case of the transistor and the ambient air.

According to (1), for a given load resistance R_L the maximum power dissipation per output transistor depends only on the supply voltage V_{CC}. In order not to exceed the permissible dissipation, the following relation must be satisfied

$$V_{CC} \leq \sqrt{\frac{\overline{R_L P_P}}{K_D}}$$

$$V_{CC} \leq K_C\sqrt{R_L P_P}, \tag{4}$$

where

$$K_C = \frac{1}{\sqrt{K_D}} \text{ (see Table I).}$$

The maximum power output $P_{0\max}$ of a transistor power amplifier is given by

$$P_{0\max} = K_0 \frac{(V_{CC} - 2V_{CE(\min)})^2}{R_L}, \tag{5}$$

where

$V_{CC} - 2V_{CE(\min)}$ = maximum peak-to-peak output voltage.
$V_{CE(\min)}$ = minimum collector-to-emitter *on* voltage at maximum output current.
K_0 = factor given in Table I for a sine, triangular, and square waves.

In the Appendix the maximum power dissipation per output transistor is derived for a sine wave in the general case of $V_Q \neq V_{cc}/2$ and $I_Q > 0$ (20). It is shown, however, that if I_Q is much smaller than the maximum output current over the temperature range, the contribution of the quiescent current to the power dissipation is negligible. As the quiescent current is normally small, the derivations of the maximum power dissipation for a triangular wave (30) and a square wave (37) consider the case where $V_Q \neq V_{cc}/2$ but where $I_Q = 0$.

The best efficiency is obtained when the quiescent voltage is one half of the supply voltage V_{cc}. If this is not the case the power dissipation is given by (20), (30) and (37) of the Appendix instead of by (1).

Two other problems in connection with the power dissipation, for which there are several approaches, are crossover distortion and thermal instability. If the output is operated in Class C, there is no quiescent current and thus no thermal instability. The resultant distortion can be reduced by driving the output stage from a current source and by applying large feedback over the amplifier, but for reasons which will be presented in Section III, crossover distortion may still be a problem. If, as an alternative, the output transistors are operated in Class AB to eliminate crossover distortion, then thermal stability must be considered.

In a Class-AB output stage, temperature-sensitive elements such as diodes or thermistors are commonly used in the biasing network in conjunction with a resistor in each emitter. However, this type of temperature compensation is not completely effective for transient temperature changes due to power dissipation of the output transistors. Therefore, a sufficient factor of safety in this circuit requires an emitter resistance which is not small compared with the load resistance, thus reducing the amplifier efficiency. A biasing scheme which allows safe operation in Class AB without sacrificing the efficiency or the maximum power-output capability is described in Section IV.

III. Distortion in Push-Pull Transistor Amplifiers

Distortion in Class-AB and Class-C push-pull transistor amplifiers will be analyzed using Fig. 2, which is a simplified schematic of a complementary emitter-follower circuit.

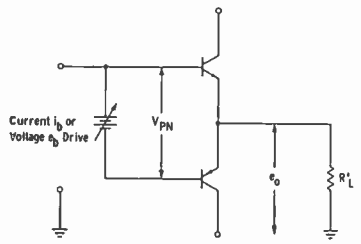

Fig. 2—Simplified complementary emitter-follower stage.

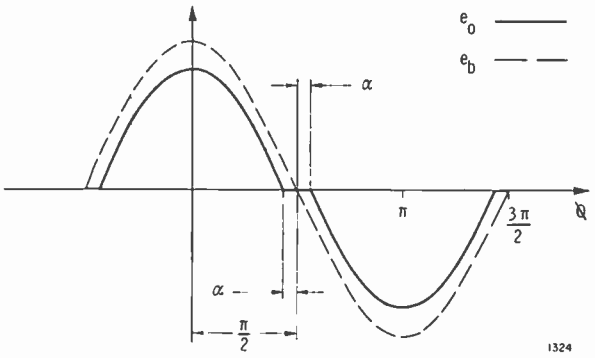

Fig. 3—Crossover distortion waveform with voltage drive.

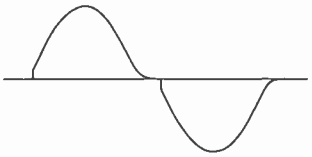

Fig. 4—Crossover distortion waveform with current drive.

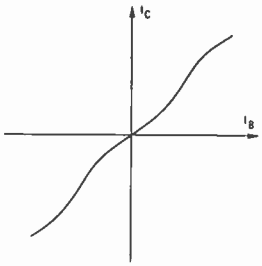

Fig. 5—I_C/I_B characteristics showing the nonlinearity due to h_{FE} variations with I_B or I_C.

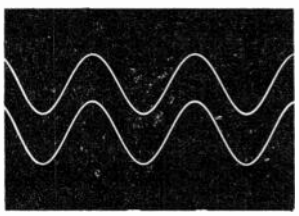

Fig. 6—Input voltage (lower) and output voltage (upper) in Class AB at I_Q=1 per cent I_P, I_P=100 ma; frequency 1 kc.

First, consider the voltage V_{PN} to be zero. In this case the amplifier will operate in Class C. A voltage source drive will give the crossover distortion shown in Fig. 3 due to nonconduction of both transistors during the period from $(\pi/2-\alpha)$ to $(\pi/2+\alpha)$. Outside of this region the output signal will be

$$e_0 = e_b - V_{BE}, \tag{6}$$

where

V_{BE} = Voltage drop from base to emitter when the transistor is on.

The variations of V_{BE} are negligible outside of the region $(\pi/2-\alpha)$ to $(\pi/2+\alpha)$ hence during the conduction period the output signal is simply a portion of a sine wave.

A current source drive will result in the output waveform shown in Fig. 4. The waveform includes two types of distortion. The nonlinearity of the I_C/I_B transfer function shown in Fig. 5 causes one type of distortion. There is also a crossover distortion that can be explained as follows: when the current i_b changes sign, there will be no output current until the base emitter capacitance charges to the V_{BE}(on) voltage.

In Class-AB operation the voltage V_{PN} is adjusted so that the transistors draw a small quiescent current. With the conduction angle greater than π and a voltage source drive, distortion will result only from variations in V_{BE}(on) which are negligible during the conduction period, as was already mentioned. However, with a current source drive, there would be no great advantage over the Class-C operation because even though the crossover distortion would disappear, there is no appreciable improvement of the I_C/I_B characteristic. The advantages of Class-AB operation are thus evident for voltage drive if a reliable bias scheme, such as discussed in detail in Section IV, is used to control quiescent current. The output waveform in Class AB with a voltage source drive and a quiescent current equal to 1 per cent of the peak ac current is compared with the input voltage in Fig. 6. (Voltage scales for the two waveforms are slightly different.)

IV. Biasing and DC Stability of a Class-AB Output Stage

The new biasing method which stabilizes the Class-AB output stage is shown in Fig. 7. The complementary phase inverter, Q_3–Q_4, is included in the biasing network.

In the analysis of the variations of I_Q as a function of V_{PN} and of the temperature T first assume R_b equals zero. The voltage V_{PN} will then be equal to the sum of the V_{BE}'s of the transistors Q_3, Q_4 and Q_5, and will have an I_Q/V_{PN} idealized characteristic as shown in Fig. 8. This characteristic is given for three different temperatures, T_1, T_2, and T_3, to show that a small variation of temperature will produce a large change in the current I_Q.

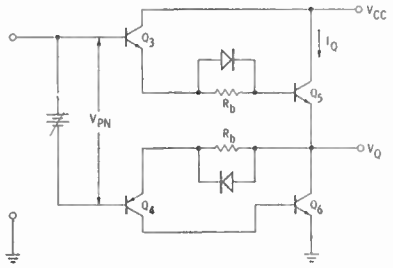

Fig. 7—Output section of amplifier with resistance diode bias network.

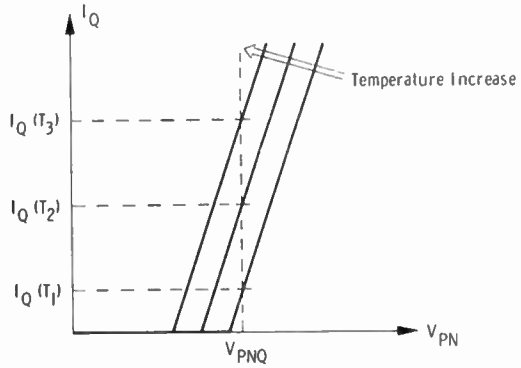

Fig. 8—Idealized characteristic of I_Q/V_{PN}.

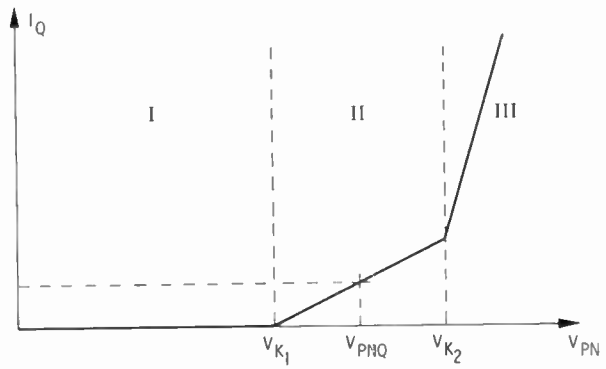

Fig. 9—New I_Q/V_{PN} characteristic resulting from the insertion of the resistance diode network.

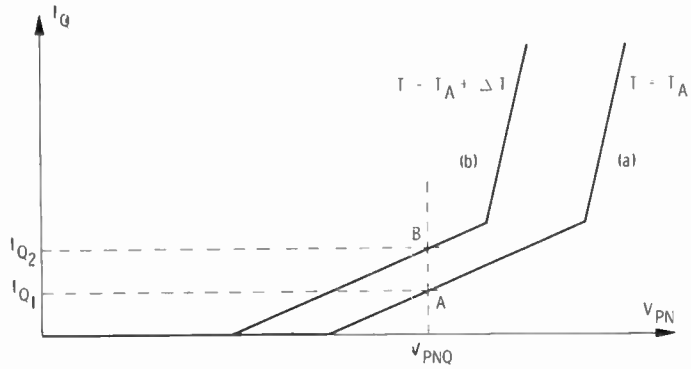

Fig. 10—Shift of the I_Q/V_{PN} characteristic due to temperature increase.

There is, therefore, an unstable condition since an increase in I_Q produces an increase in the dissipation of Q_5 and subsequently a rise in temperature which tends to raise I_Q.

The V_{BE} of a transistor varies with junction temperature T_J. This variation can be caused by both ambient temperature changes and transistor power dissipation. The ambient temperature effect is compensated by making V_{PN} equal to the forward drop V_{PNQ} of three diodes which track the thermal variation of the I_Q/V_{PN} characteristic. The dissipations in the transistors Q_3 and Q_4 are negligible. Only the dissipation in Q_5, which can raise the temperature of its junction well above the ambient, has to be taken into account. It will cause the I_Q/V_{PN} characteristic to shift to the left, producing an excessive increase in I_Q and possibly thermal runaway.

Secondly in this analysis, the resistance R_b is made greater than zero, and this resistance shunted by diodes, as shown in Fig. 7, results in the I_Q/V_{PN} characteristic of Fig. 9. The voltage V_{PNQ} across the three diodes in series should fall in region II of the characteristic. The difference $(V_{PNQ}-V_{K1})$ should be independent of temperature, but unfortunately the compensation is not perfect and a slight variation occurs (V_{K1} decreases faster than V_{PNQ} for increasing temperature).

The width of region II decreases with increasing temperature since it is determined by two diodes in series. Besides these variations it is necessary to consider the variations of the temperature of Q_5 due to power dissipation. The junction temperature of Q_5 can rise well above the ambient temperature which will cause the I_Q/V_{PN} characteristic to shift to the left. At the same time the current gain of Q_5 increases. For $R_b > 500\,\Omega$ the quiescent base current of Q_5 is practically independent of temperature.

The following procedure can be used to obtain the value of I_Q. In Fig. 10, let

T_A = ambient temperature
ΔT = increase of temperature of Q_5
$h_{FE}(T)$ = dc current gain of Q_5 at the temperature T

Curve (a) in Fig. 10 shows the I_Q/V_{PN} characteristic at ambient temperature, T_A, and curve (b) shows the same characteristic shifted by the effect of ΔT. At the ambient temperature the quiescent current is I_{Q1}—point A, curve (a). At a higher temperature, $T_A+\Delta T$, the curve is shifted by ΔV such that the new quiescent current is I_{Q2}—point B, curve (b). The quantity for ΔV is given by

$$\Delta V \simeq -2\Delta T(\text{mv/°C}),$$

where

-2 mv/°C = the temperature coefficient of the characteristic (a).

In calculating I_{Q2} it has been assumed that $h_{FE}(T_A+\Delta T)$ of Q_5 is equal to $h_{FE}(T_A)$. However, the h_{FE} of Q_5 does

vary with T; therefore, to obtain I_{Q3} at $T_A+\Delta T$, I_{Q2} must be multiplied by a correction factor ϵ.

$$\epsilon = \frac{h_{FE}(T_A + \Delta T)}{h_{FE}(T_A)}\bigg|_{I_Q=I_{Q3}} \tag{7}$$

and

$$I_{Q3} = \epsilon I_{Q2}. \tag{8}$$

Since ϵ is a function of I_{Q3}, a trial-and-error method must be used to obtain the correct value. R_b is chosen to satisfy the requirement that,

$$I_{Q3} \ll \frac{V_{CC} - V_Q}{R_L}. \tag{9}$$

For example

$$I_{Q3} < 0.05\,\frac{V_{CC} - V_Q}{R_L}.$$

V. A 10-Watt Audio Amplifier

The circuit shown in Fig. 11 is a variation of the basic design[1] used in most transformerless transistor power amplifiers. The emitter-follower stage Q_1 provides a high input impedance to the amplifier. Common-emitter stage Q_2 supplies the dc bias for the output section by means of the three diodes D_1, D_2 and D_3. They are in series with the collector resistance which is bootstrapped to increase the available voltage swing beyond the power-supply voltage, V_{CC}. Complementary emitter followers Q_3 and Q_4 (see Fig. 2) in Class AB provide a low impedance drive to the load $R_L' \simeq h_{FE}R_L$. However, n-p-n power transistors Q_5 and Q_6 are necessary to supply the output current required into the load, R_L. The gain is given by

$$A \simeq -\frac{Y_s}{Y_f} \simeq -\frac{R_f}{R_s}$$

(See Appendix.)

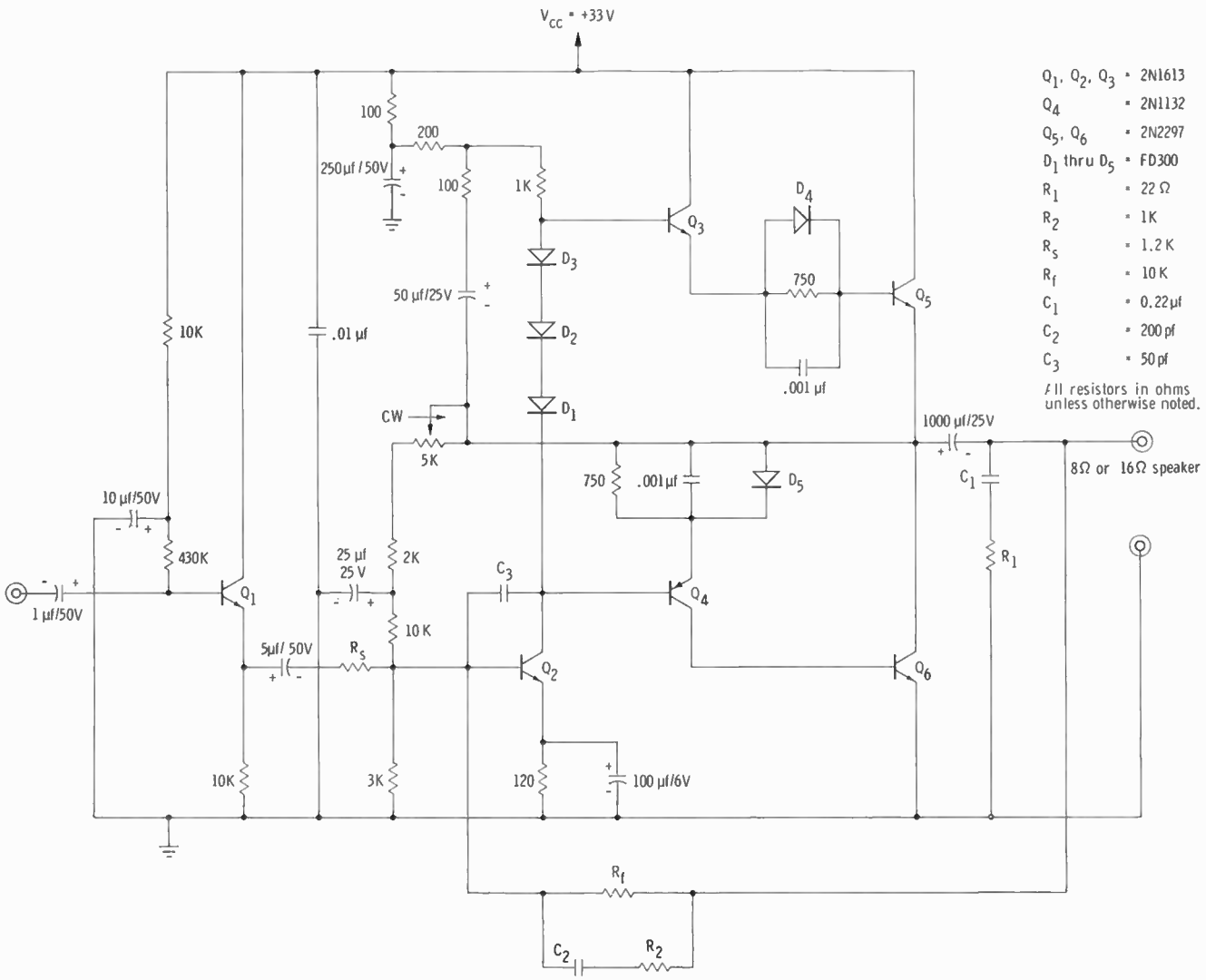

Fig. 11—10-watt audio power amplifier.

[1] H. C. Lin, "Quasi-complementary transistor amplifier," *Electronics*, vol. 29, pp. 173–175; September, 1956.

The series resistor-capacitor combination R_1C_1 at the amplifier output corrects the phase of the feedback at high frequency for the inductive load offered by a loudspeaker. The R_2C_2 network, paralleled with R_f, and the capacitor C_3, connected from base-to-collector of Q_2, provide a controlled roll-off at 60 kc. DC feedback is applied through the base-bias resistance of Q_2 which stabilizes the amplifier for temperature variations. The biasing adjustment in the base of Q_2 is set for V_Q (dc voltage at the emitter of Q_5) to be equal to $V_{CC}/2$. Therefore, the formulas of Section II can be applied. Because the amplifier is intended for sound reproduction, the coefficients in Table I for the case of a sine wave will be used.

A. Amplifier Design

1) Calculation of the permissible dissipation with the following conditions:

$T_A = 25°C$
$T_{J\max} = 200°C$
$\theta_{J-C} = 35°C/w$—for the 2N2297 transistor
$\theta_{C-A} = 15°C/w$—for a single-sided aluminum radiator with an approximate surface area of 100 cm².

Using (3),

$$P_P = \frac{T_{J\max} - T_A}{\theta_{J-C} + \theta_{C-A}} = 3.5 \text{ w.}$$

2) Calculation of the supply voltage with the following conditions:

$$R_L = 8\ \Omega$$
$$P_P = 3.5 \text{ w}$$
$$K_C = 2\pi.$$

Using (4)

$$V_{CC} \leq K_C\sqrt{R_L R_P} = 33 \text{ v.}$$

3) Calculation of the maximum power output with the following conditions:

$$R_L = 8\ \Omega$$
$$V_{CC} = 33 \text{ v}$$
$$V_{CE}(\min) = 4 \text{ v}\ ^2$$
$$K_0 = 1/8.$$

Using (5)

$$P_{0\max} = K_0 \frac{(V_{CC} - 2V_{CE}(\min))^2}{R_L} = 9.8 \text{ w}$$

[2] $V_{CE}(\min) = V_{BE}(\text{on})|_{Q_5} + V_F|_{D_4} + V_{CE}(\text{sat})|_{Q_3}$

where

$V_{BE}(\text{on})|_{Q_5}$ = base-to-emitter voltage drop of Q_5 at peak collector current.
$V_F|_{D_4}$ = voltage drop across the diode D_4 at peak output current.
$V_{CE}(\text{sat})|_{Q_3}$ = collector-to-emitter saturation voltage of Q_3 at peak output current.

B. Amplifier Performance

1) In Fig. 12, the solid line represents the amplifier-frequency response at 1-watt power output into an 8-Ω speaker load, and the dashed line represents the response at the same power output into an 8-Ω resistive load with networks R_1C_1, R_2C_2, and C_3 removed.

2) The 5-kc square wave response at 5 watts power output into an 8-Ω resistive load is given in Fig. 13.

3) The 1-kc harmonic distortion at 5 watts power output is less than 1 per cent.

4) The output impedance at 1 kc is approximately 0.5 Ω.

5) The total output noise power with the input shorted is more than 100 db below maximum rated output.

6) The power supply current vs power output is given in Fig. 14.

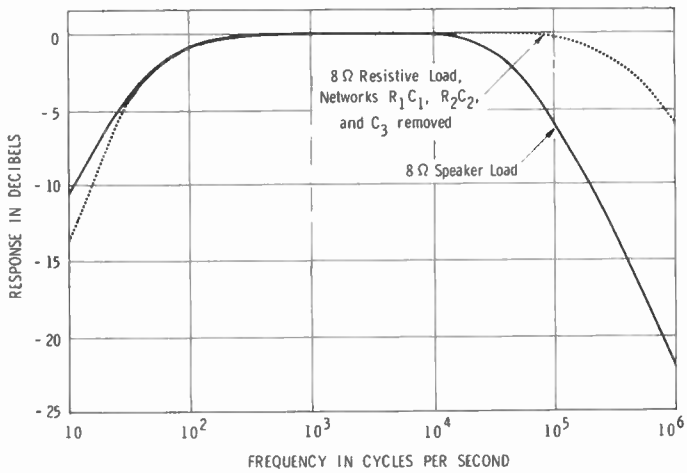

Fig. 12—Amplifier frequency response.

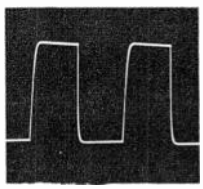

Fig. 13—Amplifier 5-kc square wave.

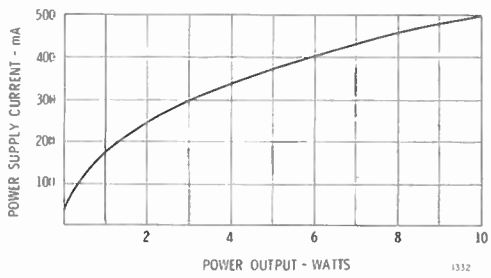

Fig. 14—Power supply current vs power output.

Appendix

A. Analysis of the Power Dissipation in the Output Transistors

Fig. 15 represents the push-pull output stage used in this analysis. In this analysis let

V_{CC} = power supply voltage
V_Q = quiescent voltage with no ac signal
I_Q = quiescent current with no ac signal
I = rms value of output current
V = rms value of output voltage

1) *Sine Wave:* For a sine wave the expressions of the collector current I_C and collector-to-emitter voltage V_{CE} of Fig. 15 are

$$I_C = I_Q + \sqrt{2}\, I \cos \phi \tag{10}$$

$$V_{CE} = V_{CC} - V_Q - \sqrt{2}\, V \cos \phi. \tag{11}$$

The average power dissipation in the upper transistor[3] is

$$P = \frac{1}{2\pi} \cdot 2 \int_0^{\phi_0} I_C V_{CE} d\phi \tag{12}$$

where ϕ_0 is defined as the angle at which $I_C = 0$ (see Fig. 16). Hence from (10)

$$I_C = 0 = I_Q + \sqrt{2}\, I \cos \phi_0$$

$$\phi_0 = \frac{\pi}{2} + \arcsin\left(\frac{I_Q}{\sqrt{2}\, I}\right) = \frac{\pi}{2} + \Delta\phi \tag{13}$$

and

$$\Delta\phi = \arcsin \frac{I_Q}{\sqrt{2}\, I}. \tag{14}$$

From (10)–(12)

$$P = \frac{1}{\pi} \int_0^{\phi_0} (I_Q + \sqrt{2}\, I \cos \phi)(V_{CC} - V_Q - \sqrt{2}\, V \cos \phi) d\phi$$

$$P = \frac{1}{\pi} (V_{CC} - V_Q) I_Q \int_0^{\pi/2+\Delta\phi} d\phi + \frac{\sqrt{2}}{\pi} [I(V_{CC} - V_Q) - V I_Q] \int_0^{(\pi/2)+\Delta\phi} \cos \phi d\phi - \frac{2}{\pi} V I \int_0^{(\pi/2)+\Delta\phi} \cos^2 \phi d\phi \tag{15}$$

$$P = \frac{1}{\pi} (V_{CC} - V_Q) I_Q \left(\frac{\pi}{2} + \Delta\phi\right) + \frac{\sqrt{2}}{\pi} [I(V_{CC} - V_Q) - V I_Q] \cos \Delta\phi - \frac{1}{\pi} V I \left(\frac{\pi}{2} + \Delta\phi - \sin \Delta\phi \cos \Delta\phi\right). \tag{16}$$

[3] The lower transistor is not considered because it has no influence on the dc stability considerations of Section IV.

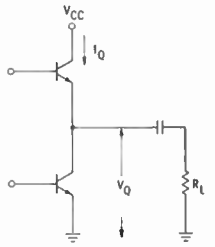

Fig. 15—Output stage of *n-p-n* power transistors.

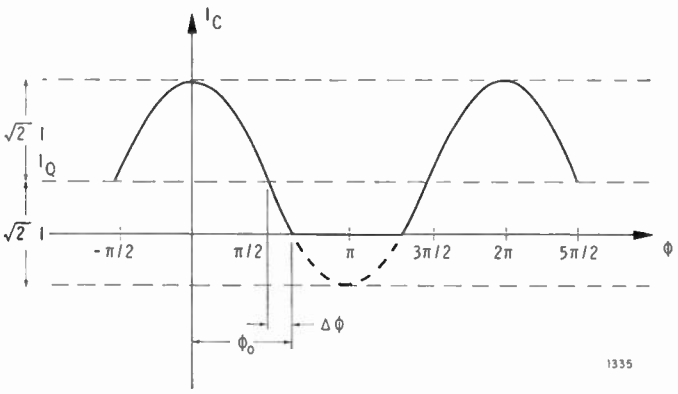

Fig. 16—Current waveform of one output transistor in Class-AB operation.

Assuming that $\Delta\phi \ll \pi/2$ the following approximations may be made

$$\sin \Delta\phi = \Delta\phi$$

$$\cos \Delta\phi = 1$$

and replacing I by V/R_L, the average power dissipation becomes

$$P = -\frac{V^2}{2R_L} + \frac{\sqrt{2}}{\pi} \cdot \frac{V}{R_L} (V_{CC} - V_Q - I_Q R_L) + \frac{1}{2} I_Q (V_{CC} - V_Q). \tag{17}$$

Differentiating with respect to V,

$$\frac{dP}{dV} = -\frac{V}{R_L} + \frac{\sqrt{2}}{\pi R_L} (V_{CC} - V_Q - I_Q R_L).$$

For

$$V = \frac{\sqrt{2}}{\pi} (V_{CC} - V_Q - I_Q R_L) = V_1,$$

$$\left.\frac{dP(V)}{dV}\right|_{V_1} = 0 \quad \text{and} \quad \frac{d^2P(V)}{dV^2} < 0. \tag{18}$$

Therefore, V_1 corresponds to the maximum average power dissipation which has the value

$$P(V_1) = P_{D\max} = -\frac{1}{\pi^2 R_L}(V_{CC} - V_Q - I_Q R_L)^2 + \frac{2}{\pi^2 R_L}(V_{CC} - V_Q - I_Q R_L)^2 + \frac{1}{2} I_Q (V_{CC} - V_Q)$$

$$P_{D\max} = \frac{1}{\pi^2 R_L}[(V_{CC} - V_Q)^2 - 2(V_{CC} - V_Q) I_Q R_L + I_Q^2 R_L^2] + \frac{1}{2} I_Q (V_{CC} - V_Q)$$

$$P_{D\max} = \frac{1}{\pi^2} \cdot \frac{(V_{CC} - V_Q)^2}{R_L} + I_Q \left[0.3(V_{CC} - V_Q) + \frac{I_Q R_L}{\pi^2} \right]. \quad (19)$$

Since R_L is always small ($\leq 50\ \Omega$), for small values of I_Q the term $I_Q R_L/\pi^2$ may be neglected and $P_{D\max}$ becomes the simple expression

$$P_{D\max} = 0.11 \frac{(V_{CC} - V_Q)^2}{R_L} + 0.3 I_Q (V_{CC} - V_Q). \quad (20)$$

To justify the assumption that $\Delta\phi \ll \pi/2$ at the level $P(V_1)$, I is replaced in (14) by V_1/R_L,

$$\sin \Delta\phi = \frac{I_Q R_L}{\sqrt{2}\, V_1}.$$

Introducing the value of V_1 from (18)

$$\sin \Delta\phi = \frac{\pi}{2} \cdot \frac{I_Q}{\frac{V_{CC} - V_Q}{R_L} - I_Q},$$

but for any practical application, the quiescent current should be much smaller than the peak current, *i.e.*,

$$\frac{V_{CC} - V_Q}{R_L} \gg I_Q, \quad (21)$$

so that $\sin \Delta\phi \ll 1$ and $\sin \Delta\phi \simeq \Delta\phi$. Under this assumption, the quiescent current I_Q has a small contribution to $P_{D\max}$. The first term of (20) is the most important limitation to the power supply voltage V_{CC}.

2) *Triangle Wave*: For a triangular wave, neglecting the quiescent current I_Q, (Fig. 17)

$$V_{CE} = (V_{CC} - V_Q) - V\left(1 - 4\frac{t}{T}\right) = V_0 - V\left(1 - 4\frac{t}{T}\right) \quad (22)$$

$$I_C = \frac{V}{R_L}\left(1 - 4\frac{t}{T}\right) \quad (23)$$

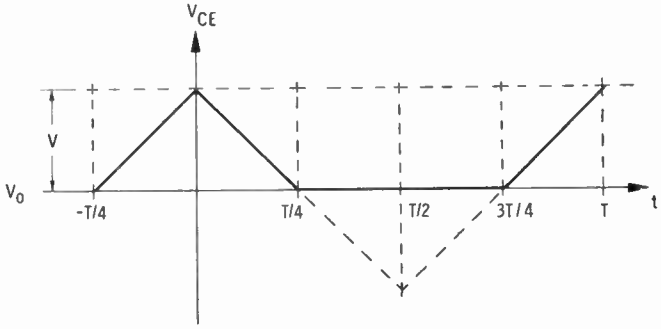

Fig. 17—Voltage waveform across one of the output transistors in Class-B operation (triangular output).

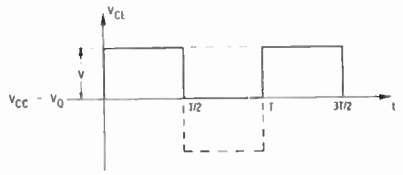

Fig. 18—Voltage waveform across one of the output transistors in Class-B operation (square wave output).

$$V_{CE} I_C = \frac{V_0 V}{R_L} - \frac{V^2}{R_L} + 4\frac{V}{R_L}(2V - V_0)\frac{t}{T} - 16\frac{V^2}{R_L}\cdot\frac{t^2}{T^2} = A + B\frac{t}{T} + C\frac{t^2}{T^2} \quad (24)$$

$$P = \frac{2}{T}\int_0^{T/4} V_{CE} I_C dt = \frac{2}{T}\int_0^{T/4}\left(A + \frac{B}{T}t + \frac{C}{T^2}t^2\right)dt = \frac{1}{2}A + \frac{1}{16}B + \frac{2}{3\times 4^3}C \quad (25)$$

$$P = \frac{1}{2}\cdot\frac{V}{R_L}(V_0 - V) + \frac{1}{4}\cdot\frac{V}{R_L}(2V - V_0) - \frac{1}{6}\cdot\frac{V^2}{R_L} \quad (26)$$

$$P = \frac{1}{4}\cdot\frac{V}{R_L}V_0 - \frac{1}{6}\cdot\frac{V^2}{R_L}. \quad (27)$$

Differentiating with respect to V,

$$\frac{dP}{dV} = \frac{1}{4}\cdot\frac{V_0}{R_L} - \frac{1}{3}\cdot\frac{V}{R_L}. \quad (28)$$

For

$$V = V_1 = \frac{3}{4}V_0, \quad (29)$$

$$\left.\frac{dP}{dV}\right|_{V=V_1} = 0 \quad \text{and} \quad \frac{d^2P}{dV^2} < 0.$$

Therefore, V_1 corresponds to the maximum power dissipation which has the value,

$$P_{D\max} = \frac{3}{32}\cdot\frac{V_0^2}{R_L} = \frac{3}{32}\cdot\frac{(V_{CC} - V_Q)^2}{R_L}. \tag{30}$$

If

$$V_{CC} - V_Q = V_{CC}/2,$$

$$P_{D\max} = \frac{3}{128}\cdot\frac{V_{CC}^2}{R_L}. \tag{31}$$

3) *Square Wave:* For a square wave, neglecting the quiescent current, I_Q, (Fig. 18)

$$V_{CE} = V_{CC} - V_Q - V \tag{32}$$

$$I_C = \frac{V}{R_L} \tag{33}$$

$$P = \frac{1}{2}\cdot V_{CE}I_C = \frac{1}{2}\left[\frac{V_{CC} - V_Q}{R_L}V - \frac{V^2}{R_L}\right]. \tag{34}$$

Differentiating power with respect to V,

$$\frac{dP}{dV} = \frac{1}{2}\cdot\frac{V_{CC} - V_Q}{R_L} - \frac{V}{R_L} \tag{35}$$

$$\frac{dP}{dV} = 0 \text{ gives } V = \frac{V_{CC} - V_Q}{2}, \tag{36}$$

and therefore

$$P_{D\max} = \frac{1}{8}\cdot\frac{(V_{CC} - V_Q)^2}{R_L}. \tag{37}$$

If

$$V_{CC} - V_Q = V_{CC}/2,$$

$$P_{D\max} = \frac{1}{32}\cdot\frac{V_{CC}^2}{R_L}. \tag{38}$$

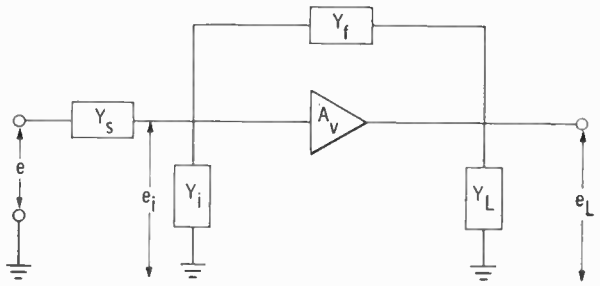

Fig. 19—General feedback amplifier.

B. Derivation of Amplifier Gain Equation

A general feedback amplifier is shown in Fig. 19, Y_i is the input admittance of the amplifying device, Y_L is the load admittance, A_V is the voltage gain of the device and Y_f and Y_s are the gain determining elements. The equations representing the amplifier are

$$(e - e_i)Y_S + (e_L - e_i)Y_f - e_iY_i = 0 \tag{39}$$

$$e_i = e_L/A_V. \tag{40}$$

Solving (39) and (40)

$$eY_S + e_LY_f\left(1 - \frac{Y}{A_VY_f}\right) = 0,$$

where

$$Y = Y_S + Y_f + Y_i.$$

Therefore

$$A = \frac{e_L}{e} = -\frac{Y_S}{Y_f}\cdot\frac{1}{1 - \dfrac{Y}{A_VY_f}}. \tag{41}$$

If $A_VY_f \gg Y$, (41) becomes

$$A = -\frac{Y_S}{Y_f}. \tag{42}$$

Electron Microscopy Studies of the Surfaces of Magnetic Recording Media*

F. NESH† AND D. B. BALLARD†

Summary—**A technique has been developed for replicating the surfaces of magnetic recording media. The media used included new magnetic tape, used magnetic tape, and "Hypalon" disks; this latter material is used in recording belts. Magnifications ranged from 10,000× to 80,000× direct magnification, and up to 240,000× by photographic enlargement. The electron micrographs thus obtained show a very much smaller unit crystal size for γ-ferric oxide than previously supposed. There is also an apparent relationship between the magnetic properties and the dispersion and unit particle size of the iron oxide particles on the tape surface.**

Introduction

A PREVIOUS study,[1] conducted in this laboratory, on the chemical and physical properties of magnetic recording tape resulted in effects which could be explained only by the particulate nature of the surface. Consequently, electron microscopy studies were indicated. These were undertaken first to study the surfaces of three commercially obtained tapes. Six photomicrographs were made, two of each tape, at 10,000× and 40,000× direct magnification. These are new unused tapes and are shown in Figs. 1 through 6. Figs. 1 and 2 both show tape G, at 10,000× and 40,000× direct magnification, respectively; Figs. 3 and 4 show tape D at 10,000× and 40,000 direct magnification, respectively; and Figs. 5 and 6 show tape C at 10,000× and 40,000× direct magnification, respectively.[1]

Figs. 7 through 14 are a result of a study of magnetic recording disks made of "Hypalon" with γ-ferric oxide dispersed throughout.

Finally, a micrograph was made of used tape as compared to new tape. This is shown in Fig. 16.

Procedure

The procedure for obtaining one-step negative replicas from recording tapes was as follows:

1) A one-inch length of tape was secured to a glass microscope slide with two small pieces of transparent adhesive tape.
2) The slide was placed in a belljar and a vacuum of 10^{-5} mm Hg was produced.
3) Palladium was deposited first at 45° (with respect to the surface plane of the tape) and then carbon was deposited at 90°.
4) Small squares, large enough to cover a 2.3-mm grid were cut from the shadowed tape and immersed in a spot plate depression which had been filled with acetone.
5) The detached polyester backing was removed and the acetone was replaced with a 50 per cent solution of HCl several times until all the Fe_2O_3 particles were dissolved.
6) The acid residue was washed away with distilled H_2O which contained a few drops of acetone.
7) The replica was then picked up on a 200-mesh copper grid, and mounted in a holder for examination in the Siemens Elmiskop 1.

Negative two-step replicas of the "Hypalon" Recording Disk were made in the following manner:

1) The highly compressed surface of the "Hypalon" Disk was first etched with 10 per cent Nital as examination of the untreated surface did not show structural detail. In order to examine the structure immediately below the surface, approximately 0.001 inch thickness of material was sliced with a razor blade parallel to the recording surface.
2) These surfaces were then covered with a 2 per cent Formvar or 4 per cent Parlodian solution.
3) The thoroughly dried plastic was stripped from the disk with transparent adhesive tape after flexing the disk several times. The use of Formvar or Parlodian did not always allow a satisfactory replica to be stripped from the disk as all plastics tested had a tendency to adhere to the freshly cut "Hypalon."
4) The replica was first shadowed with Palladium at 45°, then backed with Carbon at 90°.
5) The Formvar was removed with ethylene dichloride, and the Parlodian with amyl acetate, using the Jaffee method. Then the remaining replica was mounted on 200-mesh copper grid for examination in the electron microscope.

Discussion

The tapes shown in Figs. 1 through 6 were saturated in the center of a magnetizing coil by a dc field of 500 oersteds and a 60-cycle ac field of 600 oersteds. The remanent merit (Maxwells/mg/cm)[1] of tape "G" is 0.61 as compared to 0.46 for tape C and 0.44 for tape D. This could not be explained by any chemical impurity or chemical doping. Figs. 1, 3, and 5 show the surfaces of

* Received December 7, 1962.
† National Bureau of Standards, Washington, D. C.
[1] F. Nesh and R. F. Brown, Jr., "A study of the chemical and physical properties of magnetic recording tape," IRE TRANS. ON AUDIO, vol. AU-10, pp. 70–71; May–June, 1962.

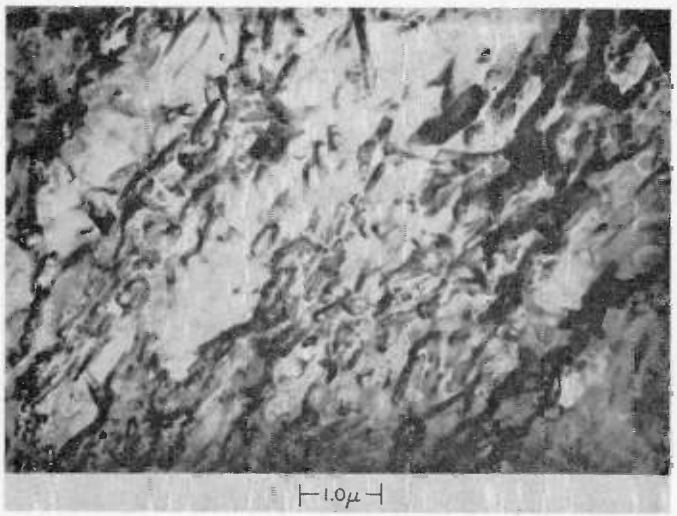

Fig. 1—A replica of the surface of tape G at 10,000× direct magnification.

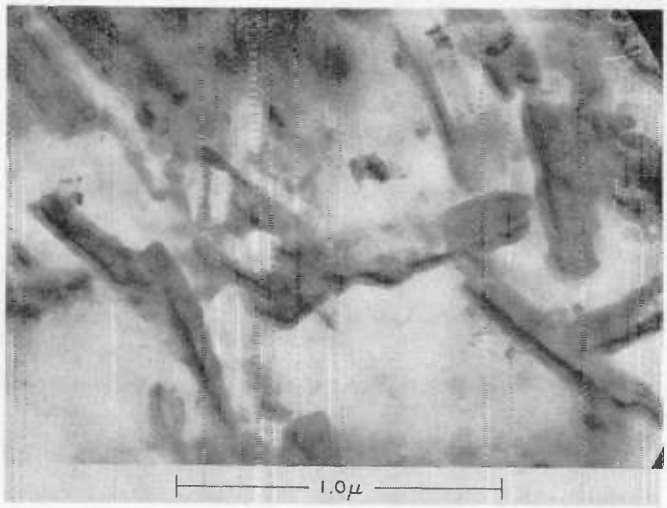

Fig. 2—A replica of the surface of tape G at 40,000× direct magnification.

Fig. 3—A replica of the surface of tape D at 10,000× direct magnification.

Fig. 4—A replica of the surface of tape D at 40,000× direct magnification.

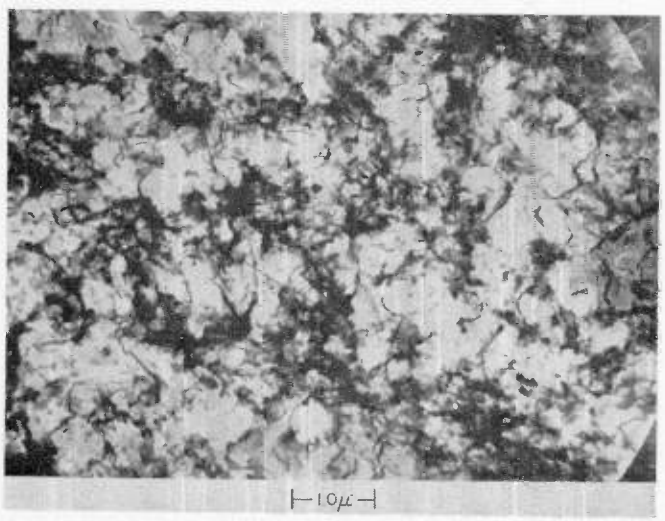

Fig. 5—A replica of the surface of Tape C at 10,000× direct magnification.

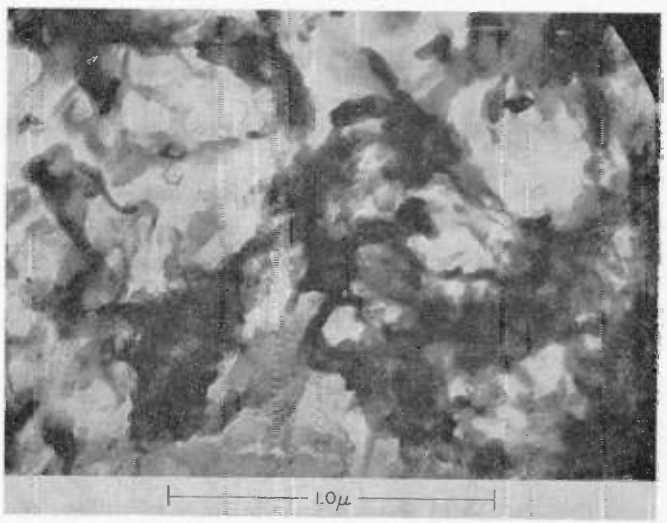

Fig. 6—A replica of the surface of tape D at 40,000× direct magnification.

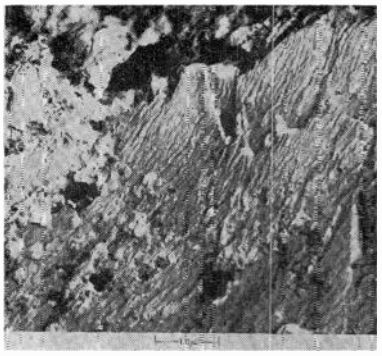

Fig. 7—A replica of the surface of a portion of "Hypalon" recording material sliced parallel to and just below the recording surface at 10,000× direct magnification.

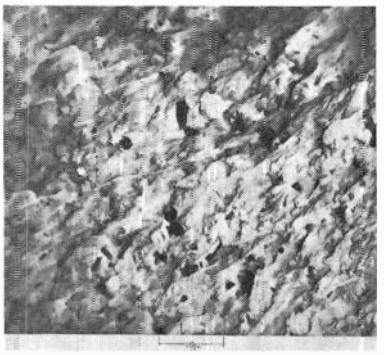

Fig. 8—A replica of the surface of a portion of "Hypalon" recording material sliced parallel to and just below the recording surface at 10,000× direct magnification.

Fig. 9—A replica of an etched portion of the surface of "Hypalon" recording material at 20,000× direct magnification.

Fig. 10—A replica of an etched portion of the surface of "Hypalon" recording material at 40,000× direct magnification.

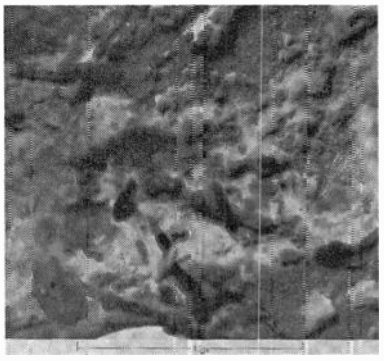

Fig. 11—A replica of an etched portion of the surface of "Hypalon" recording material at 40,000× direct magnification.

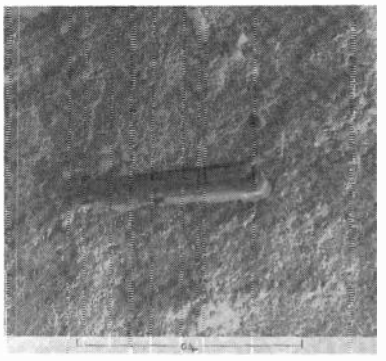

Fig. 12—A replica of a crystal packet on the etched surface of "Hypalon" recording material at 60,000× direct magnification.

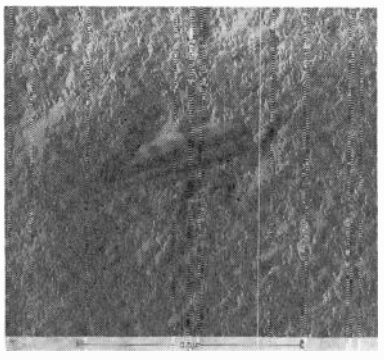

Fig. 13—A replica of a crystal packet on the etched surface of "Hypalon" recording material at 80,000× direct magnification.

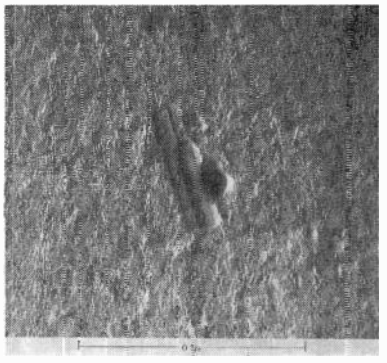

Fig. 14—A replica of a crystal packet on the etched surface of "Hypalon" recording material at 80,000× direct magnification.

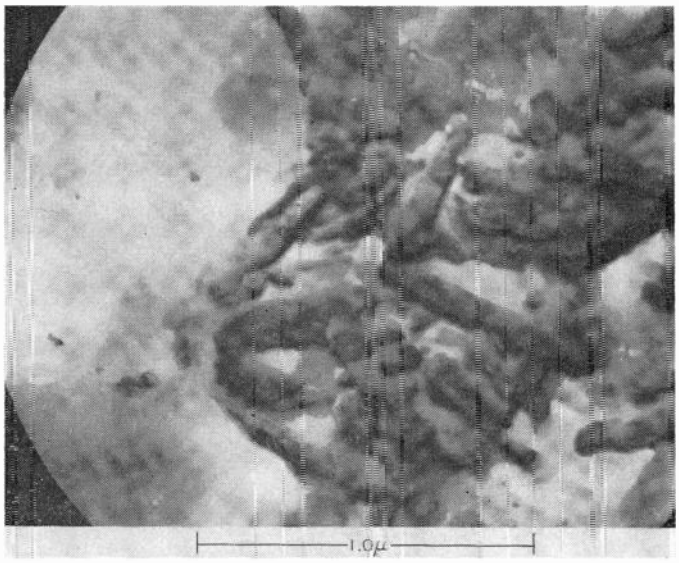

Fig. 15—A replica of the surface of tape G, previously demagnetized, at 40,000× direct magnification.

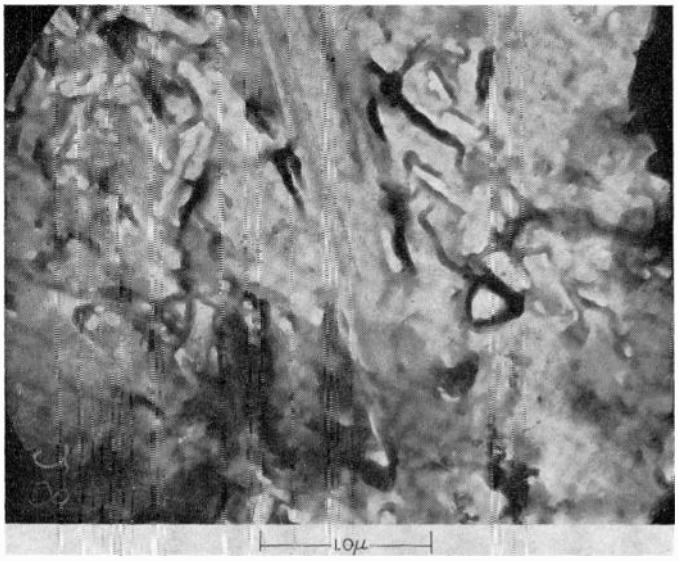

Fig. 16—A replica of the surface of used tape of the same class as tape G at 20,000× direct magnification.

tapes G, D, and C, respectively, at 10,000× direct magnification. Tape C shows a very thick, very clumped iron oxide coating; tape D shows a somewhat thinner but far better dispersed coating; tape G shows, in addition to a thinner and better dispersed coating, a distinct orientation which can be seen to be not only in a favored direction but also somewhat perpendicular. Figs. 2, 4, and 6 show the surfaces of the same tapes at 40,000× direct magnification. Even at this high magnification tape C shows nothing but clumps while tape G shows the best dispersion with the smallest unit particle size. Tape C, in addition to having the lower remanent merit along with tape D, also resists magnetization greatly at low field strengths, which is to be expected from the clumped state of its coating.

Figs. 7 through 14 represent various studies on a disk of "Hypalon" belting material. Fig. 7 is a portion sliced parallel to and just below the polished recording surface with a direct magnification of 10,000×. It shows a rough synthetic rubber surface with no apparent evidence of iron oxide particles being present. Fig. 8 is another area from the same specimen used in Fig. 7, also at 10,000× direct magnification. This area shows the furrowed effect of oriented γ-Fe_2O_3 particles; also some stripped Fe_2O_3, carbon black and other particles. Fig. 9 is a replica of an etched portion of the surface in which the γ-Fe_2O_3 particles were loosened and stripped from the eroded surface with the replica. The magnification is 20,000× direct. Fig. 10 is a higher magnification, 40,000× direct, of the same area shown in Fig. 8. It shows the replicas of γ-Fe_2O_3 imbedded in the plastic and stripped carbon black appearing as opaque particles on the surface. Fig. 11 is a replica of an eroded area from the nital treated surface at 40,000× direct magnification. It shows the eroded plastic surface, replicas of some γ-Fe_2O_3 particles and some stripped particles released by the erosion. Fig. 12 is a replica of an isolated crystal packet on the nital treated surface at 60,000× direct magnification. At lower magnification this packet appeared to be a single crystal. Here one can see at least five crystals in the packet. Fig. 13 shows a crystal packet still partially imbedded in the plastic, 80,000× direct magnification; and Fig. 14, also 80,000× direct magnification, a packet consisting of at least three crystals. The total size of the smallest crystal in the picture is 0.3 μ by 0.025 μ where 0.015 μ is due to the palladium-carbon coating, indicating a probable crystal size of 0.3 μ by 0.01 μ. Also, the crystals are apparently blunt-edged and not acicular.

Fig. 15 is a replica at 40,000× direct magnification of a sample of tape G which had been demagnetized in the coil. This shows the same appearance as the saturated sample.

Fig. 16 shows the surface of a used sample of a tape of the same class as tape G at 20,000× direct magnification. This sample had been subject to 41 plays and 41 rewinds. It shows the effects of wear, and possibly frictionally produced heat, on the tape surface. The particles and plastic have a rough appearance rather than being smoothly dispersed as in the unused samples. Also there is a rut across the tape as if made by a microscopic clump of Fe_2O_3 particles that had come off and adhered to the head and had scratched the tape.

Conclusion

Replication techniques have been developed which clearly show the structure and dispersion of magnetic particles in recording media. They show a unit rod-shaped crystal of at least 0.3-μ by 0.01-μ size, if not possibly smaller.

The results indicate improved magnetic properties with increased dispersion and smaller unit particle size.

A Simple Logarator
(Logarithmic Compressor)*

PAUL W. KLIPSCH†, SENIOR MEMBER, IRE

Summary—**A circuit comprising rectifiers, diodes and incandescent lamps as nonlinear resistors, and linear resistors to produce a dc output proportional to the largest of one or more ac inputs has been devised. It is capable of a linear range of more than 25 db with 0.5 db accuracy.**

Applications include plotting of response curves in decibels and measuring reverberation time. Two or more spaced microphones may be used under reverberant conditions to minimize effects of standing wave nulls or to simulate binaural hearing.

LOGARITHMIC converters and compressors have been built using servodrives and logarithmic potential dividers, and also with nonlinear circuit elements. Most of these are complex, involve maintenance of moving parts and wear on sliding resistors and are expensive.

The present logarithmic converter was designed primarily for testing loudspeaker response where a range of 20 db would be considered adequate. One sought for feature was to be able to use 2 or more spaced microphones and measure the average or the output of whichever microphone is in the most intense field. As Snow[1] suggests, speaker performance in a "normal environment" is more significant than under anechoic conditions, but room standing wave patterns result in deep nulls which reduce usefulness of the recorded response curves.

A considerable amount of literature exists wherein it is pointed out that the standing wave effect may be reduced by warbled frequencies, paddle wheel air movers, swinging or rotating microphones, etc. Snow's suggestion was to record 2 or more microphones, not as a phasor sum but as a scalor sum, or whichever is the larger. Choice of source and load impedances in the circuit of Fig. 1 will enable one to record the average of several sources, or whichever is the largest. As employed, the source impedances are of the order of 1 ohm, the load about 200 ohms, so the tendency is for the load circuit to be at the voltage of the largest source voltage; other sources at a lower voltage do not feed current to the load.

A priori limits were not set in the design of the converter, except that it was felt that at least 20-db range should be sought, and the ability to use 2 or more sources would be desirable.

The first idea tried was the simple compressor which lacked adequate range. Solid state diodes seemed to afford as much control as thermionic diodes. Addition of a nonlinear resistor in the form of an incandescent lamp[2] extended the volume range.

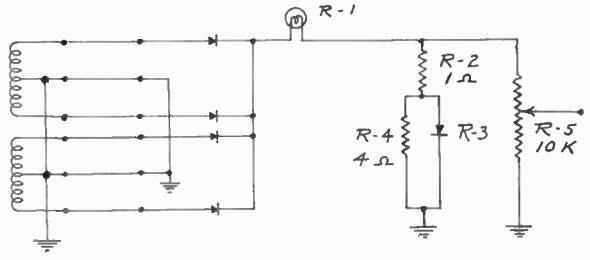

Fig. 1—Coils at left represent transformer secondaries of amplifier (altered to put center taps at ground potential). The amplifier was "stereo" providing 2 signals. Circuit at right indicates log converter or "Logarator." R-1 consists of 3 incandescent lamps, GE 27, in series; R-3 is a Sarkes-Tarzian 40-H diode. The rectifiers may be the same. The resistor values shown may be altered to fit requirements.

Fig. 1 shows the circuit as constructed. This is capable of operating out of any audio power amplifier in which the center taps of the output transformers may be grounded. So far all amplifiers tried have permitted this modification. If the output transformer secondary is part of the negative feedback loop, grounding the center tap instead of one end will reduce the feedback 6 db and permit distortion to increase, but the rectified logarithmic converter is itself a high distortion device so a slight increase in distortion in the amplifier is of no significance.

Fig. 2 shows the accuracy of the experimental unit. The points are measured 2 db steps input and volts output. The "line of best fit" through the points indicates errors of considerably less than 0.5 decibel over more than a 25-db range.

In Fig. 3, the solid curve indicates qualitatively the "response" of a diode; the series-connected lamps pass more current when cold and tend to fill up the dip in the "a" region; the series resistor R-2 lifts the output in the "b" range. The proportioning of the lamp and resistor values is done by "cut and try." If a range exceeding about 25 db is needed, a more sophisticated arrangement of several diodes with bias potential would be needed.

* Received October 1, 1962; revised manuscript received December 3, 1962.

† Klipsch and Associates, Inc., Hope, Ark.

[1] W. B. Snow, "Loudspeaker testing in rooms," *J. Audio Engr. Soc.*, vol. 9, pp. 54–60; January, 1961.

[2] The first application of an incandescent lamp for a comparable purpose appears to have been to an audio oscillator. F. E. Terman, R. R. Buss, W. R. Hewlett and F. C. Cahill, "Some applications of negative feedback with particular reference to laboratory equipment," PROC. IRE, vol. 37, pp. 649–655; September, 1939.

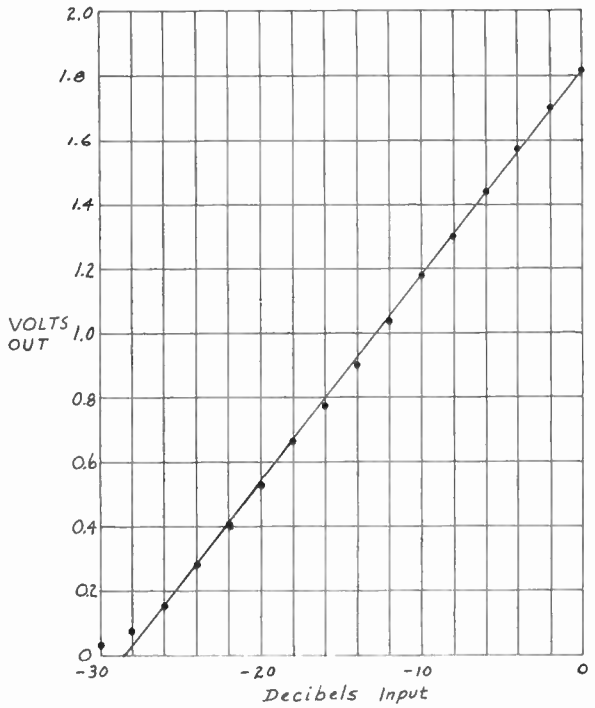

Fig. 2—Output in dc volts vs input in decibels of circuit of Fig. 1. The points are measured; the straight line is a "line of best fit" over a 26-db range. Zero db level is approximately 15-volts rms each side of center tap.

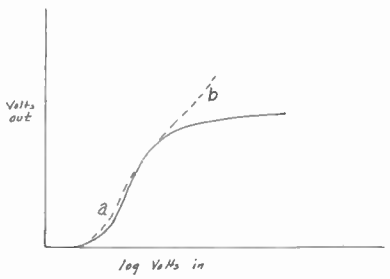

Fig. 3—Qualitative response of various elements; solid curve, dc output vs db input of diode only; curve a, effect of incandescent lamps (R-1); curve b, effect of linear resistor R-2 in Fig. 1. Further straightening of curve was accomplished with R-4.

Frequency response of the over-all system shows a drop of 2 db at the range extreme of 20,000 cps, and this coincides with the amplifier response so the compressor system may be said to be free of frequency response errors up to 20 kc.

Thermal lag in the incandescent lamp causes a 1-db overshoot for large (15 db) step changes of input. It has not yet been tried for reverberation time measurements, but it is believed to be potentially useful if the thermal lag and *X-Y* recorder inertia effects are taken into account. These effects could be minimized by tape recording the events at 15 ips and playing them back at 7.5 or 3.75 ips for plotting the decay on an *X-Y* or *X-T* recorder.[3]

The 3-decade frequency range and 25-db volume range have proved more than adequate for loudspeaker testing. The cost of the compressor parts was of the order of $35; the amplifier was a "hi fi stereo" amplifier retailing at the $190 level, and modified only to the extent of moving ground connections from one end of the output coils to the 4-ohm center taps.

The *X-Y* recorder used was a Houston Instrument Company HR 921. The oscillator was a Hewlett-Packard HO-2-207A. Sweep times (20–20,000 cps) of the order of 50–60 sec were found to give good detail; room effects may be reduced by using a sweep time of 30 sec. The recorder response speed is the limitation rather than the "logarator" system. The particular recorder requires a negative dc voltage with respect to "ground" to provide deflection in the desired direction. The circuit shown may be poled in either direction simply by poling all the individual diodes.

The name is obviously coined; the system is not properly a "compressor" since the output waveform does not correspond to the input, which is rectified and somewhat smoothed. "Logarator" seems to suggest a device for taking the logarithm of some input signal.

[3] J. M. Eargle, private communication.

A Study of the Field Around Magnetic Heads of Finite Length*

IBRAHIM ELABD†

Summary—This paper gives a determination of the field around magnetic heads of finite lengths and infinite permeability. The conventional Schwartz-Christoffel [3] transformation was used to map the inside of the polygon, corresponding to a finite magnetic head, into the upper half of the w plane. The mapping equation was derived and the equipotential lines, corresponding to a particular head-to-gap length ratio, were calculated.

The equipotential lines for the same ratio were determined experimentally using the analog field plotter. A comparison of the two sets of curves shows that they are in fair agreement, the discrepancy being due to inaccuracy in the experimental measurements.

Finally, the study includes a brief discussion of how the use of magnetic heads of finite lengths would increase the packing density of recorded pulses in both RZ and NRZ types of recording.

Introduction

THE FIELD around the semi-infinite head, shown in Fig. 1 has been calculated by Westmijze [1] using the Schwartz-Christoffel transformation and by Fan [2] using Fourier integrals.

The head configuration of Fig. 1, however, departs a great deal from the actual shape of the heads used nowadays for magnetic recording. Such heads are usually shaped as shown in Fig. 2, having finite lengths.

This paper gives a theoretical study of the field around the finite heads shown in Fig. 3. This configuration gives a better approximation of the actual heads than the one used by both Westmijze and Fan.

Throughout this work the permeability (u) of the heads is assumed to be infinite, at least for frequencies not too high. This is justified because modern heads are made of high-μ materials.

Theoretical Analysis

Since u is ∞, the boundaries of the head represent equipotential lines and the y axis is a zero equipotential line because of symmetry. We must now find the equipotential lines that lie between the head and the y axis. It is sufficient to consider the lines between half the head and the y axis.

Let the magnetic potential at any point (x, y) be ϕ.

Therefore, $\phi=0$ for $x=0$ (y axis) and $\phi=$const (ϕ_c) along the boundary of the head; that is, $\phi=\phi_c$ for $x=h_1$ and $0<y<-j\infty$, $\phi=\phi_c$ for $h_1<x<h_2$ and $y=0$ and $\phi=\phi_c$ for $x=h_2$ and $0<y<-j\infty$.

It is now required to map the inside of the polygon $(a_o, a_1, a_2, a_3, a_0)$ in Fig. 4 into the upper half of the w plane shown in Fig. 5 by the use of the Schwartz-Christoffel transformation.

The equation for the transformation is

$$z = z_0 + a\int w^{-1}(w-1)^{1/2}(w-\lambda)^{1/2}dw.$$

Now let $f=(w-1)(w-\lambda)$; hence,

$$z = z_0 + a\int \frac{\sqrt{f}}{w}\,dw.$$

But, as shown in Appendix I,

$$\int \frac{\sqrt{f}}{w}\,dw = \sqrt{f} - \log\left\{\left[\sqrt{f}+w-\frac{1+\lambda}{2}\right]^{(1+\lambda)/2} \cdot\left[\frac{\sqrt{f}+\sqrt{\lambda}}{w}-\frac{1+\lambda}{2\sqrt{\lambda}}\right]^{\sqrt{\lambda}}\right\}.$$

Hence,

$$z = z_0 + a\sqrt{f} - a\log\left\{\left[\sqrt{f}+w-\frac{1+\lambda}{2}\right]^{(1+\lambda)/2} \cdot\left[\frac{\sqrt{f}+\sqrt{\lambda}}{w}-\frac{1+\lambda}{2\sqrt{\lambda}}\right]^{\sqrt{\lambda}}\right\}. \quad (1)$$

Where z_o and a are complex quantities, let $a=a_r+ja_i$, and $z_o=z_{or}+jz_{oi}$. Thus, it is necessary to find the values of the constants a_r, a_i, z_{or}, z_{oi} and λ. It should be noted that λ must be real and greater than 1, since it maps a point that follows the point (h_1, o) in the z plane. The values of these constants are determined by substituting the values of w at the points b_1, b_2 and b_3 in (1) for z and then comparing the obtained values of z from (1) with the values of z at a_1, a_2 and a_3. This is done in Appendix II.

If $h_2/h_1=c$, then the values of the constants are found to be

$$\lambda = (2c^2-1) + 2c\sqrt{c^2-1} \quad (2)$$

$$a_r = o \quad (3)$$

$$a_i = -\frac{h_1}{\pi(c+\sqrt{c^2-1})} \quad (4)$$

$$z_{or} = h_1(1+c) \quad (5)$$

$$z_{oi} = -\frac{h_1}{\pi}\left[c\log\left((c^2-1)+c\sqrt{c^2-1}\right) + \log\sqrt{c^2-1}\right]. \quad (6)$$

* Received October 9, 1962. This work was done with the cooperation of the Research Department, Ampex Corporation, Redwood City, Calif.

† University of Alexandria, Alexandria, Egypt.

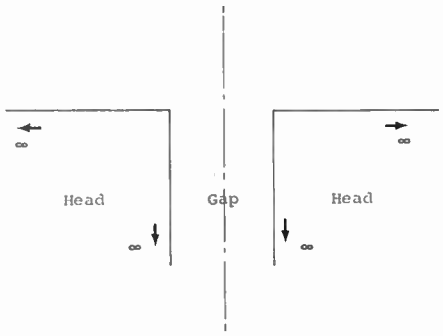

Fig. 1.

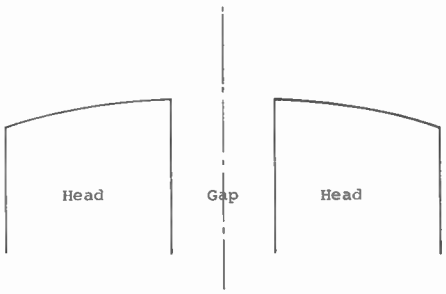

Fig. 2

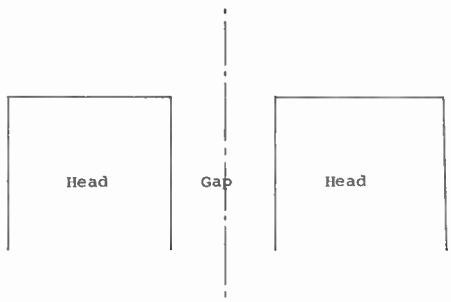

Fig. 3.

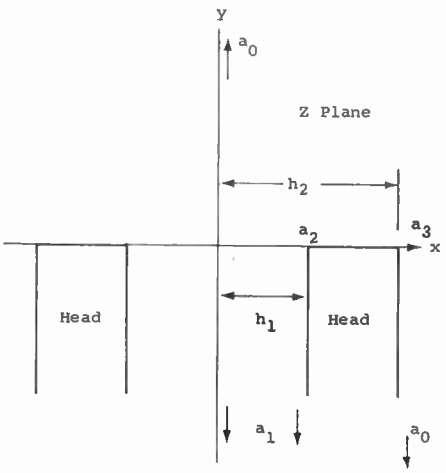

Fig. 4.

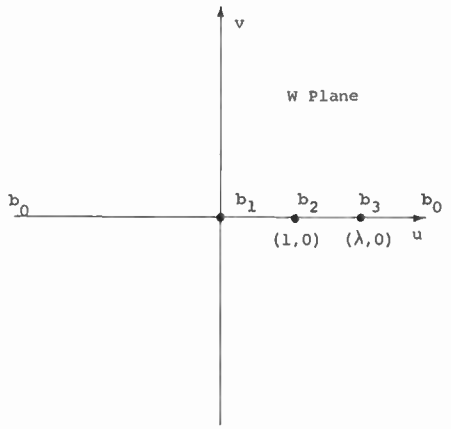

Fig. 5.

Thus, the final mapping equation is

$$z = h_1(1+c) - \frac{jh_1}{\pi}\left[c\log\left((c^2-1)+c\sqrt{c^2-1}\right)+\log\sqrt{c^2-1}\right]$$
$$-\frac{jh_1}{\pi(c+\sqrt{c^2+1})}\left[\sqrt{w^2-(2c^2+2c\sqrt{c^2-1})w+(2c^2-1)+2c\sqrt{c^2-1}}\right]$$
$$+\frac{jh_1}{\pi}\left\{c\log\left[\sqrt{w^2-(2c^2+2c\sqrt{c^2-1})w+(2c^2-1)+2c\sqrt{c^2-1}}+w-c^2-c\sqrt{c^2-1}\right]\right.$$
$$\left.+\log\left[\frac{\sqrt{w^2-(2c^2+2c\sqrt{c^2-1})w+(2c^2-1)+2c\sqrt{c^2-1}}}{w}+\frac{c+\sqrt{c^2-1}}{w}-c\right]\right\}. \qquad (7)$$

This equation is valid for any value of c that makes λ real and is greater than 1, *i.e.*, for values of c greater than 1 and less than infinity.

In the w plane, the positive half of the u axis is an equipotential line $\phi=\phi_c$ and the negative half is an equipotential line $\phi=0$. The equipotential lines are radial lines from the origin, as shown in Fig. 6. The magnetic field lines are concentric semicircles with the origin as center. The magnetic field and equipotential lines can be determined in the z plane by substituting different values of w on any of these lines in the mapping equation and obtaining the corresponding values of z, which would lie on the corresponding line in the z plane.

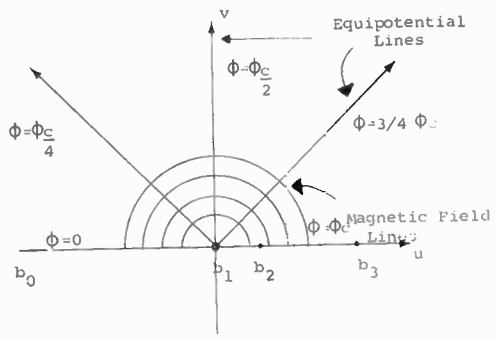

Fig. 6.

Experimental Results

A special case was considered with $c=3$, *i.e.*, equal gap and head lengths. The equipotential lines were calculated using (7). They were traced experimentally for this particular case using resistive paper and the analog field plotter. Both the theoretical and the experimental lines are shown in Fig. 7 together with the equipotential lines for the semi-infinite configuration obtained by Westmijze [1].

A comparison of the experimental and theoretical lines shows that they are in fair agreement. The discrepancy is caused by the errors in the experimental results. These errors are partially due to the fact that the resistive tracing paper was not infinite, but mainly to the fact that the potential away from the gap is a very sensitive function of its position within the gap.

Away from the gap, the field of the semi-infinite head configuration is quite different from the field of the finite head, as can be seen from Fig. 7. The difference cannot be neglected for finite head-to-gap ratios. These curves then show the large degree of disparity between the fields surrounding semi-infinite and finite magnetic recording heads, especially for finite head-to-gap ratios.

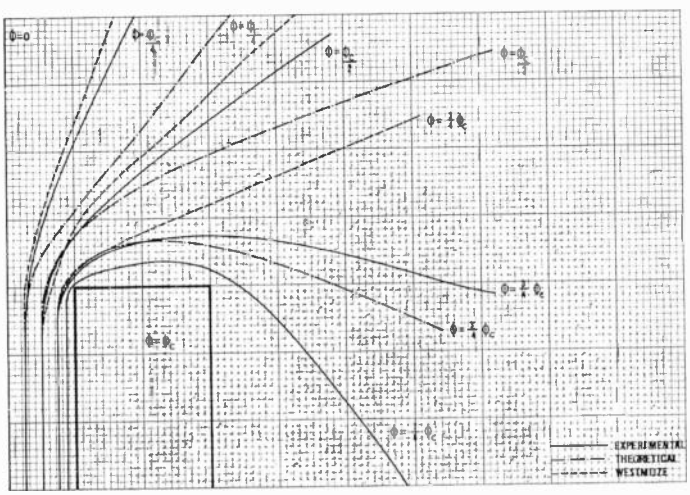

Fig. 7.

Conclusion

When a short RZ pulse is fed to a semi-infinite recording head, the shape of the pulse magnetization recorded on the tape is as shown in Fig. 8. When recorded by a finite head as shown in Fig. 9, the width is, of course, decreased, thus permitting an increase in packing density on the tape. This is true for either RZ or NRZ types of recording.

The width of the recorded pulse magnetization is determined by the characteristics of the recording heads and the magnetic medium. Knowledge of the tape characteristics will make it possible to theoretically determine the pulse shape (as done for the semi-infinite head [4]) and compare it with the experimental results obtained using a slightly different model [5] for the finite head. Such a theoretical analysis would lead to the study of different field configurations for the purpose of obtaining optimum packing densities.

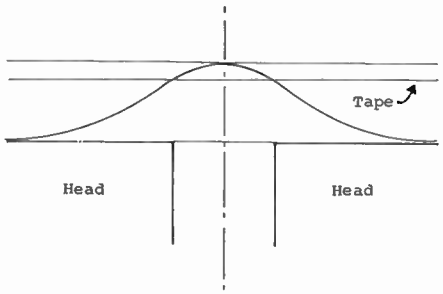

Fig. 8.

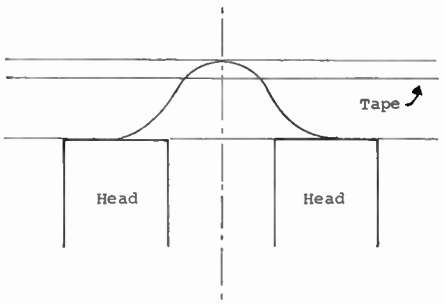

Fig. 9.

Appendix I

It is required to evaluate the integral

$$\int \frac{\sqrt{(w-1)(w-\lambda)}}{w}\,dw = \int \frac{\sqrt{w^2-(1+\lambda)w+\lambda}}{w}\,dw$$

$$= \sqrt{w^2-(1+\lambda)w+\lambda} - \frac{1+\lambda}{2}\log\left[\sqrt{w^2-(1+\lambda)w+\lambda}+w-\frac{1+\lambda}{2}\right]$$

$$= \sqrt{\lambda}\log\left[\frac{\sqrt{w^2-(1+\lambda)w+\lambda}+\sqrt{\lambda}}{w}-\frac{1+\lambda}{2\sqrt{\lambda}}\right]$$

If $f=(w-1)(w-\lambda)$, then [5]

$$\int \frac{\sqrt{f}}{w}\,dw = \sqrt{f} - \frac{1+\lambda}{2}\log\left[\sqrt{f}+w-\frac{1+\lambda}{2}\right] - \sqrt{\lambda}\log\left[\frac{\sqrt{f}+\sqrt{\lambda}}{w}-\frac{1+\lambda}{2\sqrt{\lambda}}\right]$$

$$= \sqrt{f} - \log\left\{\left[\sqrt{f}+w-\frac{1+\lambda}{2}\right]^{(1+\lambda)/2}\cdot\left[\frac{\sqrt{f}+\sqrt{\lambda}}{w}-\frac{1+\lambda}{2\sqrt{\lambda}}\right]^{\sqrt{\lambda}}\right\}.$$

Appendix II

It is required to determine the constants a_r, a_i, z_{or}, z_{oi} and λ in the mapping equation

$$z = z_{or}+jz_{oi}+(a_r+ja_i)\sqrt{f} - (a_r+ja_i)\log\left[\left(\sqrt{f}+w-\frac{1+\lambda}{2}\right)^{(1+\lambda)/2}\cdot\left(\frac{\sqrt{f}+\sqrt{\lambda}}{w}-\frac{1+\lambda}{2\sqrt{\lambda}}\right)^{\sqrt{\lambda}}\right].$$

A. At Point b_2 in w Plane

$w=(1, o)$; then, $f=0$ and $\sqrt{f}=0$. This point is the point, in the mapping of a_2 in z plane, at which $z=h_1+jo$;

$$z = (z_{or}+jz_{oi}) - [(a_r+ja_i)]\left[\log\left\{\left(1-\frac{1+\lambda}{2}\right)^{(1+\lambda)/2}\left(\sqrt{\lambda}-\frac{1+\lambda}{2\sqrt{\lambda}}\right)^{\sqrt{\lambda}}\right\}\right].$$

Therefore,

$$h_1+jo = (z_{or}+jz_{oi}) - [(a_r+ja_i)]\cdot\left[\log\left\{\left(\frac{1-\lambda}{2}\right)^{(1+\lambda)/2}\left(\frac{\lambda-1}{2\sqrt{\lambda}}\right)^{\sqrt{\lambda}}\right\}\right]$$

$$h_1+jo = (z_{or}+jz_{oi}) - [(a_r+ja_i)]\cdot\left[\log\left\{(-1)^{(1+\lambda)/2}\left(\frac{\lambda-1}{2}\right)^{(1+\lambda)/2}\left(\frac{\lambda-1}{2\sqrt{\lambda}}\right)^{\sqrt{\lambda}}\right\}\right].$$

By equating real and imaginary numbers in both sides of the equation, we obtain

$$h_1 = z_{or} - a_r\,\mathrm{Re}\left[\log\left\{(-1)^{(1+\lambda)/2}\left(\frac{\lambda-1}{2}\right)^{(1+\lambda)/2}\left(\frac{\lambda-1}{2}\right)^{\sqrt{\lambda}}\right\}\right] + a\,\mathrm{Im}\left[\log\left\{(-1)^{(1+\lambda)/2}\left(\frac{\lambda-1}{2}\right)^{(1+\lambda)/2}\left(\frac{\lambda-1}{2\sqrt{\lambda}}\right)^{\sqrt{\lambda}}\right\}\right] \quad (8)$$

and

$$o = z_{oi} - a_i\,\mathrm{Re}\left[\log\left\{(-1)^{(1+\lambda)/2}\left(\frac{\lambda-1}{2}\right)^{(1+\lambda)/2}\left(\frac{\lambda-1}{2}\right)^{\sqrt{\lambda}}\right\}\right] - a_r\,\mathrm{Im}\left[\log\left\{(-1)^{(1+\lambda)/2}\left(\frac{\lambda-1}{2}\right)^{(1+\lambda)/2}\left(\frac{\lambda-1}{2\sqrt{\lambda}}\right)^{\sqrt{\lambda}}\right\}\right] \quad (9)$$

where Re means real and Im is imaginary.

B. At Point b_3 in w Plane

$w=(\lambda, o)$; then, $f=0$ and $\sqrt{f}=0$. This point is the point, in the mapping of a_3 in the z plane, at which $z=h_2+jo$;

$$z = (z_{or}+jz_{oi}) - [(a_r+ja_i)]\cdot\left[\log\left\{\left(\lambda-\frac{1+\lambda}{2}\right)^{(1+\lambda)/2}\left(\frac{\sqrt{\lambda}}{\lambda}-\frac{1+\lambda}{2\sqrt{\lambda}}\right)^{\sqrt{\lambda}}\right\}\right].$$

Therefore,

$$h_2 + jo = (z_{or} + jz_{oi}) - [(a_r + ja_i)]\left[\log\left\{\left(\frac{\lambda-1}{2}\right)^{(1+\lambda)/2}\left(\frac{\lambda-1}{2\sqrt{\lambda}}\right)^{\sqrt{\lambda}}\right\}\right]$$

$$h_2 + jo = z_{or} + jz_{oi} - [(a_r + ja_i)] \cdot \left[\log\left\{\left(\frac{\lambda-1}{2}\right)^{(1+\lambda)/2}\left(\frac{\lambda-1}{2\sqrt{\lambda}}\right)^{\sqrt{\lambda}}(-1)^{\sqrt{\lambda}}\right\}\right].$$

By equating real and imaginary numbers in both sides of the equation, we obtain

$$h_2 = z_{or} - a_r \operatorname{Re}\left[\log\left\{(-1)^{\sqrt{\lambda}}\left(\frac{\lambda-1}{2}\right)^{(1+\lambda)/2}\left(\frac{\lambda-1}{2\sqrt{\lambda}}\right)^{\sqrt{\lambda}}\right\}\right] + a_i \operatorname{Im}\left[\log\left\{(-1)^{\sqrt{\lambda}}\left(\frac{\lambda-1}{2}\right)^{(1+\lambda)/2}\left(\frac{\lambda-1}{2\sqrt{\lambda}}\right)^{\sqrt{\lambda}}\right\}\right] \quad (10)$$

and

$$o = z_{oi} - a_i \operatorname{Re}\left[\log\left\{(-1)^{\sqrt{\lambda}}\left(\frac{\lambda-1}{2}\right)^{(1+\lambda)/2}\left(\frac{\lambda-1}{2\sqrt{\lambda}}\right)^{\sqrt{\lambda}}\right\}\right] - a_r \operatorname{Im}\left[\log\left\{(-1)^{\sqrt{\lambda}}\left(\frac{\lambda-1}{2}\right)^{(1-\lambda)/2}\left(\frac{\lambda-1}{2\sqrt{\lambda}}\right)^{\sqrt{\lambda}}\right\}\right]. \quad (11)$$

By subtracting (8) from (10), we obtain

$$\begin{aligned} h_2 - h_1 = & - a_r \operatorname{Re}\left[\log\left\{(-1)^{\sqrt{\lambda}}\left(\frac{\lambda-1}{2}\right)^{(1-\lambda)/2}\left(\frac{\lambda-1}{2\sqrt{\lambda}}\right)^{\sqrt{\lambda}}\right\}\right] \\ & + a_r \operatorname{Im}\left[\log\left\{(-1)^{(1+\lambda)/2}\left(\frac{\lambda-1}{2}\right)^{(1+\lambda)/2}\left(\frac{\lambda-1}{2\sqrt{\lambda}}\right)^{\sqrt{\lambda}}\right\}\right] \\ & + a_i \operatorname{Im}\left[\log\left\{(-1)^{\sqrt{\lambda}}\left(\frac{\lambda-1}{2}\right)^{(1+\lambda)/2}\left(\frac{\lambda-1}{2\sqrt{\lambda}}\right)^{\sqrt{\lambda}}\right\}\right] \\ & - a_i \operatorname{Im}\left[\log\left\{(-1)^{(+\lambda)/2}\left(\frac{\lambda-1}{2}\right)^{(1+\lambda)/2}\left(\frac{\lambda-1}{2\sqrt{\lambda}}\right)^{\sqrt{\lambda}}\right\}\right]. \end{aligned}$$

Since λ is a real number and is greater than 1, then

$$\log\left(\frac{\lambda-1}{2}\right)^{(1+\lambda)/2} \quad \text{and} \quad \log\left(\frac{\lambda-1}{2\sqrt{\lambda}}\right)^{\sqrt{\lambda}}$$

are real numbers. Thus, the expression for $h_2 - h_1$ simplifies to

$$\begin{aligned} h_2 - h_1 = & - a_r \operatorname{Re}\left[\log(-1)^{\sqrt{\lambda}}\right] \\ & + a_r \operatorname{Re}\left[\log(-1)\frac{1+\lambda}{2}\right] \\ & + a_i \operatorname{Im}\left[\log(-1)^{\sqrt{\lambda}}\right] \\ & - a_i \operatorname{Im}\left[\log(-1)\frac{1+\lambda}{2}\right]. \end{aligned}$$

By substituting $e^{j\pi}$ for (-1) in the above expression, we obtain

$$\begin{aligned} h_2 - h_1 = & - a_r \operatorname{Re}\left[\log e^{j\pi\sqrt{\lambda}}\right] \\ & + a_r \operatorname{Re}\left[\log e^{j\pi}\frac{(1+\lambda)}{2}\right] \\ & + a_i \operatorname{Im}\left[\log e^{j\pi\sqrt{\lambda}}\right] \\ & - a_i \operatorname{Im}\left[\log e^{j\pi}\frac{(1+\lambda)}{2}\right] \end{aligned}$$

or

$$h_2 - h_1 = - o + o + a_i\pi\sqrt{\lambda} - a_i\pi\left(\frac{1+\lambda}{2}\right).$$

Then,

$$h_2 - h_1 = - a_i\pi\left(\frac{1+\lambda}{2} - \sqrt{\lambda}\right). \quad (12)$$

Therefore,

$$a_i = - \frac{h_2 - h_1}{\pi\left(\frac{1+\lambda}{2} - \sqrt{\lambda}\right)}.$$

By considering (9) and (11), we obtain

$$\begin{aligned} o = & - a_i \operatorname{Re}\left[\log\left\{(-1)^{(1+\lambda)/2}\left(\frac{\lambda-1}{2}\right)^{(1+\lambda)/2}\left(\frac{\lambda-1}{2\sqrt{\lambda}}\right)^{\sqrt{2}}\right\}\right] \\ & + a_i \operatorname{Re}\left[\log\left\{(-1)^{\sqrt{\lambda}}\left(\frac{\lambda-1}{2}\right)^{(1+\lambda)/2}\left(\frac{\lambda-1}{2\sqrt{\lambda}}\right)^{\sqrt{\lambda}}\right\}\right] \\ & - a_r \operatorname{Im}\left[\log\left\{(-1)^{(1+\lambda)/2}\left(\frac{\lambda-1}{2}\right)^{(1+\lambda)/2}\left(\frac{\lambda-1}{2\sqrt{\lambda}}\right)^{\sqrt{\lambda}}\right\}\right] \\ & + a_r \operatorname{Im}\left[\log\left\{(-1)^{\sqrt{\lambda}}\left(\frac{\lambda-1}{2}\right)^{(1+\lambda)/2}\left(\frac{\lambda-1}{2\sqrt{\lambda}}\right)^{\sqrt{\lambda}}\right\}\right]. \end{aligned}$$

By using the same procedure followed in determining (12), we obtain

$$o = - a_r\pi\left(\frac{1+\lambda}{2}\right) + a_r\pi\sqrt{\lambda}$$

or

$$o = a_r\pi\left[\frac{1+\lambda}{2} - \sqrt{\lambda}\right].$$

Therefore,

$$a_r = 0 \quad (13)$$

since

$$\left(\frac{1+\lambda}{2} - \sqrt{\lambda}\right)$$

is zero only if $\lambda = 1$.

This is not the case since λ must be greater than 1. Substituting for a_i and a_r from (12) and (13) in (8), we obtain

$$h_1 = z_{or} + a_i\pi\left(\frac{1+\lambda}{2}\right)$$

$$h_1 = z_{or} - \left[\frac{h_2 - h_1}{\pi\left(\frac{1+\lambda}{2} - \sqrt{\lambda}\right)}\right]\left[\left(\frac{1+\lambda}{2}\right)\pi\right]. \quad (14)$$

Then,

$$h_1 = z_{or} - \frac{(h_2 - h_1)(1+\lambda)}{(1+\lambda-2\sqrt{\lambda})}.$$

Therefore,

$$z_{or} = \frac{h_2(1+\lambda) - 2h_1\sqrt{\lambda}}{1+\lambda-2\sqrt{\lambda}}. \quad (15)$$

Substituting for a_i and a_r from (12) and (13) in (9), we obtain

$$o = z_{oi} - a_i\left[\left(\frac{1+\lambda}{2}\right)\log\left(\frac{\lambda-1}{2}\right) + \sqrt{\lambda}\log\left(\frac{\lambda-1}{2\sqrt{\lambda}}\right)\right].$$

Then,

$$z_{oi} = -\frac{(h_2 - h_1)}{\pi\left(\frac{1+\lambda}{2} - \sqrt{\lambda}\right)}\left\{\left(\frac{1+\lambda}{2}\right)\log\left(\frac{\lambda-1}{2}\right) + \sqrt{\lambda}\log\left(\frac{\lambda-1}{2\sqrt{\lambda}}\right)\right\}. \quad (16)$$

Now it is required to determine λ.

C. At Point b_1 in w Plane

The point $b_1 = (0, 0)$ is a singular point in the w plane and it is the mapping of the points $z = (o, -\infty)$ and $z = (h_1, -\infty)$ in the z plane. Let $w = re^{j\Theta}$. Then, $r = o$ and $\Theta = o$ are the mapping of the point $z = (h_1, -\infty)$ in the z plane and $r = o$ and $\Theta = -\pi$ (since we are approaching the origin in the w plane from the negative direction of the real axis) are the mapping of the point $z = (o, -\infty)$ in the z plane.

From (1) we have

$$z = z_0 + a\sqrt{f} - a\log\left\{\left[\sqrt{f} + w - \frac{1+\lambda}{2}\right]^{(1+\lambda)/2}\cdot\left[\frac{\sqrt{f}+\sqrt{\lambda}}{w} - \frac{1+\lambda}{2\sqrt{\lambda}}\right]^{\sqrt{\lambda}}\right\}$$

or

$$z = z_{or} + jz_{oi} + ja_i\sqrt{f} - ja_i\log\cdot\left\{\left[\sqrt{f} + w - \frac{1+\lambda}{2}\right]^{(1+\lambda)/2}\cdot\left[\frac{\sqrt{f}+\sqrt{\lambda}}{w} - \frac{1+\lambda}{2\sqrt{\lambda}}\right]^{\sqrt{\lambda}}\right\}, \quad (17)$$

but

$$\lim_{\substack{r\to 0\\ \Theta\to 0}} z = h_1 - j\infty$$

and

$$\lim_{\substack{r\to 0\\ \Theta\to 0}} \sqrt{f} = \sqrt{\lambda}$$

and

$$\lim_{\substack{r\to 0\\ \Theta\to 0}} \log\left[\sqrt{f} + w - \frac{1+\lambda}{2}\right]^{(1+\lambda)/2}$$

$$= \log\left[\sqrt{\lambda} - \frac{1+\lambda}{2}\right]^{(1+\lambda)/2}$$

$$= \log\left[(-1)^{(1+\lambda)/2}\left(\frac{1+\lambda}{2} - \sqrt{\lambda}\right)^{(1+\lambda)/2}\right]$$

$$= \log\left[e^{j\pi(1+\lambda)/2}\right]\left[\frac{1+\lambda}{2} - \sqrt{\lambda}\right]^{(1+\lambda)/2}\Bigg]$$

$$= \left(\frac{1+\lambda}{2}\right)\log\left(\frac{1+\lambda}{2} - \sqrt{\lambda}\right) + j\pi\left(\frac{1+\lambda}{2}\right). \quad (18)$$

The quantity

$$\left(\frac{1+\lambda}{2} - \sqrt{\lambda}\right)$$

is real since λ is real and greater than 1.

$$\lim_{\substack{r\to 0\\ \Theta\to 0}} \log\left[\frac{\sqrt{f}+\sqrt{\lambda}}{w} - \frac{1+\lambda}{2\sqrt{\lambda}}\right]^{\sqrt{\lambda}} = +\infty. \quad (19)$$

By substituting (18) and (19) in (17), we obtain

$$h_1 - j\infty = z_{or} + jz_{oi} + ja_i\sqrt{\lambda} - ja_i\left[\left(\frac{1+\lambda}{2}\right)\log\left(\frac{1+\lambda}{2} - \sqrt{\lambda}\right) + j\pi\left(\frac{1+\lambda}{2}\right)\right] - ja_i\infty. \quad (20)$$

By equating real numbers on both sides of (20), we obtain

$$h_1 = z_{or} + a_i\pi\left(\frac{1+\lambda}{2}\right).$$

This is the result obtained in (14) and serves as a check to the solution. Also, we have

$$\lim_{\substack{r\to 0\\ \theta\to -\pi}} z = o - j\infty$$

and

$$\lim_{\substack{r\to 0\\ \theta\to -\pi}} \sqrt{f} = \sqrt{\lambda}$$

and

$$\lim_{\substack{r\to 0\\ \theta\to -\pi}} \log\left[\sqrt{f} + w - \frac{1+\lambda}{2}\right]^{(1+\lambda)/2} = \left(\frac{1+\lambda}{2}\right)\log\left(\frac{1+\lambda}{2} - \sqrt{\lambda}\right) + j\pi\left(\frac{1+\lambda}{2}\right),$$

just as (18) and

$$\lim_{\substack{r\to 0\\ \theta\to -\pi}} \log\left[\frac{\sqrt{f}+\sqrt{\lambda}}{w} - \frac{1+\lambda}{2\sqrt{\lambda}}\right]^{\sqrt{\lambda}} = \lim_{r\to 0} \log\left[\frac{(2\sqrt{\lambda})(e^{j\pi})}{r} - \frac{1+\lambda}{2\sqrt{\lambda}}\right]^{\sqrt{\lambda}} = \lim_{r\to 0} \log\left[\frac{2\sqrt{\lambda}}{r}e^{j\pi}\right]^{\sqrt{\lambda}} = j\pi\sqrt{\lambda} + \lim_{r\to 0} \log\left[\frac{2\sqrt{\lambda}}{r}\right]^{\sqrt{\lambda}} = j\pi\sqrt{\lambda} + \infty. \quad (21)$$

By substituting (18) and (21) in (17), we obtain

$$o - j\infty = z_{or} + jz_{oi} + ja_i\sqrt{\lambda} - ja_i\left[\left(\frac{1+\lambda}{2}\right)\log\left(\frac{1+\lambda}{2} - \sqrt{\lambda}\right) + j\pi\left(\frac{1+\lambda}{2}\right)\right] + a_i\pi\sqrt{\lambda} - ja_i\infty. \quad (22)$$

By equating real numbers in (22), we obtain

$$o = z_{or} + a_i\pi\left(\frac{1+\lambda}{2}\right) + a_i\pi\sqrt{\lambda}.$$

Substituting the value of z_{or} from (14), we obtain

$$o = h_1 - a_i\pi\left(\frac{1+\lambda}{2}\right) + a_i\pi\left(\frac{1+\lambda}{2}\right) + a_i\pi\sqrt{\lambda}.$$

Therefore,

$$a_i = -\frac{h_1}{\pi\sqrt{\lambda}} = \frac{h_1 - h_2}{\pi\left(\frac{1+\lambda}{2} - \sqrt{\lambda}\right)}.$$

Thus, we have

$$\frac{h_1}{\sqrt{\lambda}} = \frac{h_2 - h_1}{\frac{1+\lambda}{2} - \sqrt{\lambda}}. \quad (23)$$

If the values of h_1 and h_2 are known, λ and, hence, all the other constants can be determined. Assume that

$$\frac{h_2}{h_1} = c. \quad \text{Then,} \quad \frac{h_1}{\sqrt{\lambda}} = \frac{h_1(c-1)}{\frac{1+\lambda}{2} - \sqrt{\lambda}};$$

then,

$$\sqrt{\lambda}(c-1) = \frac{1+\lambda}{2} - \sqrt{\lambda}; \quad \text{Then,} \quad \sqrt{\lambda}\,c = \frac{1+\lambda}{2};$$

then,

$$\lambda - 2\sqrt{\lambda}\,c - 1 = o; \quad \text{then,} \quad \sqrt{\lambda} = c \pm \sqrt{c^2-1}.$$

Since c is greater than 1 and λ must be greater than 1, then

$$\sqrt{\lambda} = c + \sqrt{c^2-1}.$$

Therefore,

$$\lambda = (2c^2 - 1) + 2c\sqrt{c^2-1}. \quad (24)$$

By substituting the value of λ from (24) in (12), (15) and (16), we obtain

$$a_i = -\frac{h_1}{\pi(c + \sqrt{c^2-1})}$$

$$z_{or} = h_1(1+c)$$

and

$$z_{oi} = -\frac{h_1}{\pi}\left[c\log(c^2 - 1 + c\sqrt{c^2-1}) + \log\sqrt{c^2-1}\right].$$

Thus, the mapping equation (7) can be written down as shown in this paper.

References

[1] W. K. Westmijze, "Studies of Magnetic Recording," Phillips Res. Lab., Eindhoven, The Netherlands, Res. Rept. No. 8; April, 1953.

[2] G. Fan, "A Study of the Playback Process of Magnetic Recording" Ampex Corp., Redwood City, Calif., Basic Dev. Rept. No. 103; December, 1960.

[3] P. H. Morse and H. Feshbach, "Methods of Theoretical Physics," McGraw-Hill Book Co., Inc., New York, N. Y., Part I; 1953.

[4] M. Barkouki and I. Stein, "Theoretical and experimental evaluations of RZ and NRZ recording characteristics," 1962 WESCON Convention Record.

[5] L. F. Shew, "High-density magnetic head design for noncontact recording," 1962 IRE International Convention Record, pt. 4, pp. 53–62.

[6] C. D. Hodgman, "Standard Mathematical Tables," Chemical Rubber Publ. Co., Cleveland, Ohio, 12th ed.; September, 1951.

Correspondence

Further Comments on "Musical Transfer Functions and Processed Music"*

Procedures I described as "synchronization by juxtaposition" in 1955[1] and thereafter, now have become commercially available for home use in a variety of tape recorders under the labels *add-a-track*, *synchro-track*, and *simul-track*. Such recorders usually confine the add-a-track function, unidirectionally, to one particular liaison of two out of four quarter tracks. The performing synchronist, in his channelizing the first and, accordingly, the second recording, should not be held under such rigid constraints. Instantaneous switch-over of the recording function from any of the two tracks to the other, without stopping and by means of a clickless single switch, becomes the primary requirement for securing continuity of the musical time reference.

Passing to the increasingly pretentious tasks of *multichannelized synchronization* (*i.e.*, adding and/or mixing more than one musical part in any required channel-combination), one can foresee two basic patterns of *synchro-mixtures*. A third part is led either to one of the two tracks, or to both. Accordingly, the instrumentation will require a third independent and complete record/playback channel, serving a third tape-track, and provided with output splitting and mixing facilities. While recording on the third track, the synchronist receives his cueing from one or both of the prerecorded dual tracks. The information thus stored on the third track can be superposed subsequently upon the prerecorded dual tracks, or led to the speakers directly during the playback. Quartets and quintets can be administered appropriately.

Because of the complexity of his tasks, the performing synchronist will need push-button facilities to erase faulty parts before substituting his juxtaposed corrections. He receives his cueing from the playback of the opposite track.[2]

Some of the aforementioned features, of course, are available in the design of high quality tape recorders, but not their entire assembly. The writer looks forward to the advent of a "Synchromaster," designed for the use of the professional musical world.

Even without the elaborate facilities of the envisioned three-channel recorder, the techniques of *rerecording* afford nice approximation. It is recalled that a single track recorder plus a stereo recorder can be used instead of an add-a-track recorder.[2] Similarly, the combination of an add-a-track-stereo recorder plus a stereo-player can be employed for producing *synchro-mixtures*. To demonstrate this principle, the writer has synchronized the two solo parts of Bach's concerto for two violins (actually played by himself on the keyboard) and mixed subsequently his piano accompaniment upon the two tracks of a second tape, as a common background to the separated violin parts. The first recording was administered in the now conventional add-a-track mode. To this output, played back through the two external speakers of a stereo-player, a live accompaniment was added on the piano. This tonal compound was picked up by the add-a-track recorder in its *stereo* recording position. It was only necessary to position carefully the five machine components (*i.e.*, two speakers, two mikes, and the piano) and to maintain a desirable loudness balance in the piano accompaniment.

Note: After the submission of the above comments, the superiority of *selective channelization* has been demonstrated as follows.

A "program," recorded on the first track, followed the melodic line of a duo piano piece without any constraint. For example, the melodically coherent and therefore alternating sequence of solo parts and tutti sections, drawn from the duo piano score of a Mozart piano concerto, appeared on the program track. Conversely, the second track served for adding the sequence of the melodically subordinate sections in corresponding alternations. In the playback all channel-reversals were *re*-reversed by manipulating a single-pole, double-throw switch serving the two speakers. Thus it was possible to direct all solo sections to Speaker I and all tuttis to Speaker II. Consequently, a synchronist enjoying the benefits of melodically designed, selective channelization, can attain satisfactory results in many, hitherto unmanageable synchronization and multisynchronization tasks.

In the above pilot study I was aided by my son Charles, a student.

ANDREW G. PIKLER
198 Laurel Hill Ave.
Norwich, Conn.

* Received on February 6, 1963. At the U.S.N. Medical Research Laboratory, Groton, Conn. The opinions expressed in this article are not necessarily the official views of the U. S. Navy.

[1] A. G. Pikler, "Synchronization of music on dual tapes," *J. Acoust. Soc. Am.*, vol. 27, p. 974; September, 1955.

[2] A. G. Pikler, "Synchronization of music by juxtaposition on dual channel tapes," *J. Acoust. Soc. Am.*, vol. 31, p. 612; June, 1959.

Contributors

Because IEEE membership records were not consolidated at publication time, the membership progressions shown below are those of IRE.

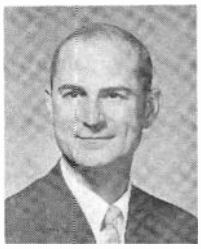

David B. Ballard was born in Shelbyville, Ind., August 29, 1924. He received the B.S. degree in metallurgical engineering from Virginia Polytechnic Institute, Blacksburg, in 1950.

He joined the Metallurgy Division of the National Bureau of Standards, Washington, D. C., in 1950. At present he is with the Metal Physics Section; for the past two years he has been concerned with the application of the Electron Microscope to studies of the microstructure of steel guage blocks, the precipitation in Dura nickel alloys, and the resultant etch pits found in a single crystal of metal etched in a molten salt.

Mr. Ballard is a member of the American Vacuum Society, ASM and Electron Microscopy Society of America.

❖

Larry Blaser (S'61–M'62) was born in Columbus, Neb., on October 3, 1931. He received the B.S.E.E. degree from the University of Nebraska, Lincoln, in 1961.

He served in the U. S. Air Force from 1953 to 1957. During 1957 and 1958 he worked for the Electronic Research Laboratory of the Lockheed Aircraft Corporation, Burbank, Calif., where he assisted in the evaluation of airborne electronic systems. In 1959 he joined the Applications Department of Fairchild Semiconductor, a division of Fairchild Camera and Instrument Corporation, Mountain View, Calif., where he has since been primarily engaged in analog circuit design. He has studied the noise properties of transistors and has developed new noise measurement techniques. He has worked on FM receiving systems and other communication circuits and has been a consultant in these areas.

❖

Donald F. Eldridge (A'50–M'55–SM'60) was born in Passaic, N. J., on January 30, 1929. He received the B.S.E.E. degree from Lehigh University, Bethlehem, Pa., in 1949.

He then joined the Boeing Airplane Co., Seattle, Wash., where he was engaged in work covering many phases of dynamic data acquisition and reduction. In 1956 he became affiliated with the Research Division of Ampex Corporation, Redwood City, Calif., where he did research on many aspects of magnetic recording. His last position there was Head of the Magnetics Department of the Ampex Corporate Research Division, from which he resigned in December, 1960. He is presently Vice President and Technical Director of Memorex Corporation, Santa Clara, Calif.

Mr. Eldridge is a member of AIP, SMPTE and AAAS. In 1961 he received the PGA Senior Award.

❖

Ibrihim Elabd, biography and photograph not available at time of publication.

Heitor Franco was born in Lisbon, Portugal, on April 2, 1932. He received the degree of Engineer in Physics from the Ecole Polytechnique de l'Universite de Lausanne, Switzerland, in 1955.

He headed the X-ray Department of Applied Research Laboratories, Inc., Lausanne, from 1959 to 1960, where he was engaged in the design and production of X-ray and spectroscopic equipment. He was a member of the Engineering Staff of the Allen B. DuMont Division of Fairchild Camera and Instrument Corporation, Clifton, N. J., between 1960 and 1962, where he designed and developed a new series of fully transistorized oscilloscopes. In 1962, he transferred to Fairchild Semiconductor, a division of the same Corporation, Mountain View, Calif., and became a member of the Applications Department, where he is engaged in device evaluation.

❖

Paul W. Klipsch (A'34–M'44–SM'45) for a photograph and biography please see page 178 of the November/December, 1962, issue of these TRANSACTIONS.

❖

Florence Nesh, for a photograph and biography please see page 90 of the May/June, 1962, issue of these TRANSACTIONS.

INSTITUTIONAL LISTINGS

The IEEE Professional Technical Group on Audio is grateful for the assistance given by the firms listed below, and invites application for Institutional Listing from other firms interested in Audio Technology.

BALLANTINE LABORATORIES, INC., Boonton, N.J.
AC Voltage Measuring Instruments (0.01 cps-1000 Mc), Laboratory Voltage Standards (0-1000 Mc)

JAMES B. LANSING SOUND, INC., 3249 Casitas Ave., Los Angeles 39, Calif.
Loudspeakers and Transducers of All Types

JENSEN MANUFACTURING CO., Div. of The Muter Co., 6601 S. Laramie Ave., Chicago 38, Ill.
Loudspeakers, Reproducer Systems, Headphones and Accessories

KNOWLES ELECTRONICS, INC., 10545 Anderson Place, Franklin Park, Ill.
Miniature Magnetic Microphones and Receivers

NATIONAL TAPE SERVICE, INC., 1259 Rt. 46, Parsippany, N.J.
Magnetic Tape Duplicating

SHURE BROTHERS, INC., Evanston, Ill.
Microphones, Phonograph Pickups, Magnetic Recording Heads, Acoustic Devices

UNITED TRANSFORMER CORP., 150 Varick St., New York, N.Y.; 3630 Eastham Dr., Culver City, Calif.
Transformers, Inductors, Electric Wave Filters, High Q Coils, Magamps, Pulse Units—Stocks & Specials

Charge for listing in six consecutive issues of the TRANSACTIONS—$75.00.
Application for listing may be made to the Professional Technical Groups
Secretary, The Institute of Electrical and Electronics Engineers, Inc.,
Box A, Lenox Hill Station, New York 21, N.Y.